Kent Academic Repository
Full text document (pdf)

Citation for published version

Labisko, Jim and Griffiths, Richard A. and Chong-Seng, Lindsay and Bunbury, Nancy and Maddock, Simon T. and Bradfield, Kay S. and Taylor, Michele L. and Groombridge, Jim J. (2019) Endemic, endangered, and evolutionarily significant: Cryptic lineages in Seychelles' frogs.   Biological Journal of the Linnean Society .   ISSN 0024-4066.

DOI

https://doi.org/10.1093/biolinnean/bly183

Link to record in KAR

https://kar.kent.ac.uk/71727/

Document Version

Author's Accepted Manuscript

1 **TITLE**

2 Endemic, endangered, and evolutionarily significant: Cryptic lineages in Seychelles' frogs

3 (Anura: Sooglossidae).

4 **RUNNING TITLE**

5 Cryptic diversity in the Sooglossidae

6 **AUTHORS**

7 **Jim Labisko (corresponding author – jl693@kent.ac.uk)**

8 Durrell Institute of Conservation and Ecology, School of Anthropology and Conservation,

9 University of Kent, Canterbury, Kent. CT2 7NR. UK; Island Biodiversity and Conservation, P.O.

10 Box 1348, Anse Royale, Mahé, Seychelles.

11 **Richard A. Griffiths**

12 Durrell Institute of Conservation and Ecology, School of Anthropology and Conservation,

13 University of Kent, Canterbury, Kent. CT2 7NR. UK.

14 **Lindsay Chong-Seng**

15 Plant Conservation Action group, P.O. Box 392, Victoria, Mahé, Seychelles.

16 **Nancy Bunbury**

17 Seychelles Islands Foundation, La Ciotat Building, Mont Fleuri. P.O. Box 853, Victoria, Mahé,

18 Seychelles; Centre for Ecology and Conservation, University of Exeter, Cornwall Campus,

19 Penryn, TR10 9FE, UK.

20 **Simon T. Maddock**

21 School of Biology, Chemistry and Forensic Science, Faculty of Science and Engineering,

22 University of Wolverhampton, Wulfruna Street, Wolverhampton. WV1 1LY. UK; Department

23 of Life Sciences, The Natural History Museum, Cromwell Road, London. SW7 5BD. UK;

24 Department of Genetics, Evolution and Environment, University College London, Gower

25   Street, London. WC1E 6BT. UK.; Island Biodiversity and Conservation, P.O. Box 1348, Anse

26   Royale, Mahé, Seychelles.

27   **Kay S. Bradfield**

28   Perth Zoo, South Perth, WA 6151, Australia.

29   **Michelle L. Taylor**

30   Durrell Institute of Conservation and Ecology, School of Anthropology and Conservation,

31   University of Kent, Canterbury, Kent. CT2 7NR. UK.

32   **Jim J. Groombridge**

33   Durrell Institute of Conservation and Ecology, School of Anthropology and Conservation,

34   University of Kent, Canterbury, Kent. CT2 7NR. UK.

35 **ABSTRACT**

36 Cryptic diversity that corresponds with island origin has been previously reported in the

37 endemic, geographically restricted sooglossid frogs of the Seychelles archipelago. The

38 evolutionary pattern has not been fully explored, and given current amphibian declines and

39 the increased extinction risk faced by island species, we sought to identify evolutionarily

40 significant units (ESUs) to address conservation concerns for these highly threatened anurans.

41 We obtained genetic data for two mitochondrial (mtDNA) and four nuclear (nuDNA) genes

42 from all known populations of sooglossid frog (the islands of Mahé, Praslin, and Silhouette)

43 to perform phylogenetic analyses and construct nuDNA haplotype networks. Bayesian and

44 maximum likelihood analyses of mtDNA support monophyly and molecular differentiation of

45 populations in all species that occur on multiple islands. Haplotype networks using statistical

46 parsimony revealed multiple high-frequency haplotypes shared between islands and taxa, in

47 addition to numerous geographically distinct (island-specific) haplotypes for each species. We

48 consider each island-specific population of sooglossid frog as an ESU and advise conservation

49 managers to do likewise. Furthermore, our results identify each island lineage as a candidate

50 species, evidence for which is supported by Bayesian Poisson Tree Processes analyses of

51 mtDNA, and independent analyses of mtDNA and nuDNA using the multispecies coalescent.

52 Our findings add to the growing understanding of the biogeography and hidden diversity

53 within this globally important region.

54

INTRODUCTION

From the observations of Darwin (1859) and Wallace (1869) on the Galapagos and Malay archipelagos, to MacArthur and Wilson's (1967) seminal work on the theory of island biogeography, islands have played a significant role as model biological systems, progressing our understanding of evolutionary theory, ecological processes, and biogeography (Adsersen, 1995; Warren *et al.*, 2015; Santos *et al.*, 2016). The uniqueness of island endemic species is well documented, yet island biotas are particularly vulnerable to extinction, largely due to human-driven habitat change or introduced species (Paulay, 1994; Cronk, 1997; Whittaker & Fernández-Palacios, 2007). Understanding the evolutionary relationships of insular taxa, and addressing threats to endemic island lineages are therefore key components in mitigating the loss of global biodiversity (Robertson *et al.*, 2014).

The granitic Seychelles (most of the inner islands of the group; Fig. 1) form part of an isolated continental block with mixed faunal origins, including both overwater dispersed and ancient endemic clades (Ali, 2017; Ali, 2018) that reveal varying degrees of affinity to the Afrotropical and Indomalayan realms. Recent explorations of molecular phylogenetic relationships of Seychelles herpetofauna have identified a broad partitioning of two biogeographic units; a northern group (consisting of Praslin and surrounding islands) and a southern group (comprised of Mahé, Silhouette, and surrounding islands) (Fig. 1). This pattern of differentiation is documented in studies across a range of taxa, including the geckos *Ailuronyx* (Rocha *et al.*, 2016a), *Phelsuma* (Rocha *et al.*, 2013), *Urocotyledon* (Rocha *et al.*, 2011); and the skinks *Pamelaescincus* (Valente *et al.*, 2013) and *Trachylepis* (formerly *Mabuya*) (Rocha *et al.*, 2016b). However, within this north-south biogeographic pattern, further evidence of cryptic diversity is beginning to emerge in several taxa (e.g. Rocha *et al.*, 2016b). The discovery of a previously unknown population of sooglossid frogs on the island

82   of Praslin—where the frogs had hitherto been unrecorded—and identification of this

83   population as an evolutionarily significant unit (ESU) (Taylor *et al.*, 2012) provided the

84   motivation to assess the genetic diversity of this family.

85

86   **Sooglossid frogs**

87   One of the world's most enigmatic and understudied frog families, the Sooglossidae (Noble,

88   1931) is one of only two amphibian families entirely restricted to an archipelago. Comprised

89   of two genera, each with two species: *Sooglossus sechellensis* (Boettger, 1896) and *So.*

90   *thomasseti* (Boulenger, 1909), and *Sechellophryne gardineri* (Boulenger, 1911) and *Se.*

91   *pipilodryas* (Gerlach & Willi, 2002), each are recognised as Evolutionarily Distinct and Globally

92   Endangered (EDGE) species and are placed in the Top 100 EDGE Amphibians (Isaac *et al.*,

93   2012; Zoological Society of London, 2015), and have been assessed for the IUCN Red List as

94   either Critically Endangered (*So. thomasseti*, *Se. pipilodryas*) or Endangered (*So. sechellensis*,

95   *Se. gardineri*) (IUCN SSC Amphibian Specialist Group, 2013a; IUCN SSC Amphibian Specialist

96   Group, 2013b; IUCN SSC Amphibian Specialist Group, 2013c; IUCN SSC Amphibian Specialist

97   Group, 2013d). Three of the four species occur on more than one island, with *So. thomasseti*

98   and *Se. gardineri* found on Mahé and Silhouette (Nussbaum, 1984), and *So. sechellensis* found

99   on Mahé, Silhouette, and Praslin (Nussbaum, 1984; Taylor *et al*., 2012). The fourth species,

100 *Se. pipilodryas*, is endemic to Silhouette (Gerlach & Willi, 2002).

101   Given the (i) importance of maintaining global and regional biological diversity, (ii)

102 increased extinction risk faced by island species, (iii) unabated international crisis of

103 amphibian declines, and (iv) global significance of the Sooglossidae as an evolutionarily

104 distinct group, this unique family is in urgent need of research attention. A stronger

105 knowledge base is also essential for conservation practitioners to make informed decisions

106 and manage the sooglossid populations. Following recent accounts of geographic partitioning

107 in Seychelles herpetofauna, and the identification of a novel, evolutionarily distinct

108 population of sooglossid frogs on Praslin, we hypothesise that: (1) undocumented cryptic

109 diversity exists across the three islands where these sooglossids occur, and (2) identification

110 of such diversity will correspond with biogeographic (island) origin. To test these hypotheses,

111 we reconstructed mitochondrial DNA phylogenies to explore the presence of divergent,

112 cryptic lineages; generated nuclear DNA haplotype networks to reveal phylogeographic

113 relationships; and performed species tree reconstructions using the multispecies coalescent.

114 Our results enable the identification of ESUs for conservation purposes (Moritz, 1994) and

115 further our understanding of the biogeography of the region.

116

117 **MATERIALS AND METHODS**

118 **Study site**

119 The inner islands of the Seychelles archipelago lie 4-5°S to 55-56°E in the western Indian

120 Ocean, and sit upon the Seychelles Bank, a largely submerged microcontinent of some

121 129,500 km^2 (Davies & Francis, 1964). Its flat upper section spans ca. 44,000 km^2 and lies an

122 average depth of 55 m below present sea level (bpsl), emerging from which are the granitic

123 inner islands (Davies & Francis, 1964; Matthews & Davies, 1966; Ali, 2018) (Fig. 1). The granitic

124 Seychelles are unique among oceanic islands, being composed of continental rock, and

125 formed upon separation from India ~63 Ma (Collier *et al.*, 2008; Chatterjee *et al.*, 2013).

126 Elevated, forested areas on the largest and highest islands of Mahé (154 km^2, 905 m

127 elevation), Praslin (38 km^2, 367 m elevation) and Silhouette (20 km^2, 740 m elevation) are the

128 only locations where sooglossid frogs are found.

129

Genetic sampling

Non-lethal tissue samples (toe-clips) were obtained from frogs representing each species and island population (Fig. 1; Table 1). We sequenced genes regularly utilised in amphibian phylogenetics that represented varying rates of molecular evolution. These comprised two mitochondrial DNA (mtDNA) fragments: *16S* rRNA (*16s*) and cytochrome b (*cytb*), plus fragments of four nuclear loci (nuDNA): proopiomelanocortin (*pomc*), recombination activating genes (*rag*) 1 and 2, and rhodopsin exon 1 (*rho*). Genomic DNA was extracted following manufacturer's guidelines using the Bioline Isolate Genomic DNA Kit. Sequences from all loci were amplified via standard polymerase-chain reaction (PCR). For primers and cycling conditions see Appendix S1; Table S1.1 in Supporting Information. Products from PCR were sequenced by Macrogen, Korea. We also utilised GenBank sequence data arising from Taylor *et al*. (2012) (*So. sechellensis 16s*), van der Meijden *et al.* (2007) (*Se. pipilodryas 16s*, *rag1*, *rag2*), and for outgroups used in phylogenetic analyses (Table S1.2). Novel sequence data generated by this study have been submitted to GenBank under accession numbers MK058722-70; MK058781-823; MK058825-979; MK058996-9390; MK072763-5.

Sequence alignment

Sequences were quality trimmed in SEQUENCHER v. 5.3 (Gene Codes Corporation, 2015) and cross-checked with chromatograms by eye in MEGA6 (Tamura *et al.*, 2013). MEGA6 was also employed to visually check (e.g. for stop codons and indels), edit, and align sequence data using default settings of the MUSCLE algorithm (Edgar, 2004). To remove any ambiguously aligned regions, sequence profiles were prepared via the GBLOCKS server v. 0.91b (Castresana, 2000; Talavera & Castresana, 2007). To preserve informative insertions and/or deletions, GBLOCKS parameters were set to allow gaps and less stringent flanking positions.

154   DATACONVERT 1.0 (Dyer *et al.*, n.d.), ALTER (Glez-Pena *et al.*, 2010) and FORMAT CONVERTOR

155   (Los Alamos National Security LLC, 2005-2006) were employed to convert sequence profiles

156   between required formats. SEQUENCEMATRIX v. 1.7.8 (Vaidya *et al.*, 2011) was used to

157   concatenate mtDNA sequence profiles.

158

159   **Mitochondrial phylogeny**

160   Sooglossid mtDNA sequences were analysed using Bayesian inference (BI) (Huelsenbeck *et*

161   *al.*, 2001) and maximum likelihood (ML) (Felsenstein, 1981) approaches. Partitioning schemes

162   and models of nucleotide evolution were determined independently with PARTITIONFINDER

163   v. 1.1.1 (Lanfear *et al.*, 2012) (Table S1.3). Branch lengths of alternative partitions were linked

164   and all schemes evaluated using the Akaike information criterion. Bayesian analysis was

165   performed in BEAST v. 2.3.2 (Bouckaert *et al.*, 2014) using two independent Markov chains of

166   100 million generations, sampling every 10,000 generations. BEAST input files were generated

167   using BEAUTI v. 2.3.2 (Bouckaert *et al.*, 2014). Chain convergence and all parameters were

168   checked using TRACER v. 1.6 (Rambaut *et al.*, 2014) to ensure adequate mixing and effective

169   sample size (ESS) values ≥ 200. Initial runs were used to fine-tune final analyses, and we

170   employed a relaxed lognormal clock as this approach may more accurately reflect lineage-

171   and locus-specific heterogeneity in rates of molecular evolution (Drummond *et al.*, 2006;

172   Lepage *et al.*, 2007; Heled & Drummond, 2010). As BEAST uses a molecular clock to estimate

173   the root position, no outgroup taxa were used in BI analyses (Heled & Drummond, 2010). We

174   assumed a stable environment for the Sooglossidae over recent geological time, and

175   therefore applied a constant population for tree priors. However, given our inter- and

176   intraspecific sampling we also performed phylogenetic reconstruction using the Yule model

177   tree prior. Support for internal branches was evaluated using Bayesian posterior probabilities

178   (PP), with well-supported clades indicated by PP values ≥ 0.95. LOGCOMBINER v. 2.3.2

179   (Bouckaert *et al.*, 2014) was used to combine tree files from the two independent runs, which

180   was summarised as a single maximum clade credibility tree with mean PP values after a 10%

181   burn-in using TREEANNOTATOR v. 1.8.2 (Drummond & Rambaut, 2007).

182   Maximum likelihood analyses were performed with RAXMLGUI v. 1.3.1 (Silvestro &

183   Michalak, 2012; Stamatakis, 2014) using default settings with GTRGAMMA model parameters

184   and 1,000 bootstrap replicates. Branch lengths were individually optimised for each partition.

185   The Nasikabatrachidae have been hypothesised to be the closest extant relative of the

186   Sooglossidae (Biju & Bossuyt, 2003; Frost *et al.*, 2006; Roelants *et al.*, 2007; Pyron & Wiens,

187   2011; Frazão *et al.*, 2015; Feng *et al.*, 2017) and used as an outgroup taxon in previous

188   phylogenetic analyses of sooglossid frogs (van der Meijden *et al.*, 2007; Taylor *et al.*, 2012).

189   However, GenBank derived *Nasikabatrachus sahyadrensis* sequence data rendered

190   *Sooglossus* and *Sechellophryne* non-monophyletic in initial runs. Leiopelmatoidea

191   (*Leiopelma+Ascaphus*) is widely accepted as the basal, sister lineage to all other extant

192   anurans, and we therefore applied this taxon as an outgroup using GenBank sequence data

193   arising from Irisarri *et al*. (2010) (*Leiopelma*) and Gissi *et al*. (2006) (*Ascaphus*). Support for

194   internal branches was evaluated using bootstrap support (BS) values, with well-supported

195   clades indicated by BS values ≥ 70. Bayesian and maximum likelihood phylogenies were

196   visualised using FIGTREE v. 1.4.3 (Rambaut, 2016).

197

198   **Multispecies coalescent and inferrence of population boundaries**

199   To infer underlying species trees and support a robust phylogenetic insight, we performed

200   reconstructions using the multispecies coalescent applied in the StarBEAST (*BEAST) package

201   within BEAST v. 2.4.8 (Bouckaert *et al.*, 2014). Multiple samples per lineage are recommended

202 to infer coalescent events, speciation and topology (Heled & Drummond 2010; Jockusch *et*

203 *al*., 2014; Lambert *et al*., 2015), therefore where possible we utilised composite taxa to

204 achieve coverage where only a single representative of a lineage was available. Data for

205 composites was derived from individuals arising from the same taxon and population of

206 origin, thereby meeting previously published criteria for composite taxa in amphibian studies

207 (e.g. Alonso *et al*., 2012; Jockusch *et al*., 2014; Maia-Carvalho *et al*., 2014) (Table S1.4). The

208 inclusion of variable loci such as mtDNA may exert disproportionate influence on other loci in

209 *BEAST analysis (Jockusch *et al*., 2014). Accordingly, we carried out independent analyses of

210 our mtDNA and nuDNA datasets. Partitioning schemes replicated that of our BEAST2 analyses

211 (Table S1.3). Using a relaxed lognormal clock we ran two independent Markov chains of 100

212 million generations, sampling every 1,000 generations, and applied the 'linear with constant

213 root' multispecies coalescent prior with the Yule model distribution of prior probability.

214 Mitochondrial DNA shared the same tree partition, nuDNA tree partitions were locus specific.

215 Checks on chain convergence and ESS values were performed as previously described. Clade

216 support was evaulated using PP values. Trees were visualised using FIGTREE.

217 To infer popuation boundaries and aid the identifcation of ESUs we subjected our

218 BEAST2 mtDNA phylogeny to Bayesian Poisson Tree Processes (bPTP) analysis implemented

219 via the online bPTP service (http://species.h-its.org/ptp) (Zhang *et al*., 2013). The bPTP model

220 applies two independent Poisson process classes (within- and among-species substitution

221 events) under a coalescent model by assuming gene tree branch lengths to infer

222 species/population boundaries. The bPTP analyses was run for 500 k Markov Chain Monte

223 Carlo generations, with a thinning parameter of 100, and a burn-in of 0.1. Posterior

224 probabilities of each node were assessed using maximum likelihood.

225

226   **Genetic variation**

227   MEGA6 was used to calculate nucleotide diversity, parsimony informative and variable sites,

228   and obtain inter-and intra-specific genetic *p*-distances for mtDNA, with pair-wise deletion of

229   missing sites. The PHASE algorithm (Stephens *et al.*, 2001; Stephens & Scheet, 2005)

230   implemented in DNASP v. 5.10.1 (Librado & Rozas, 2009) was used to determine heterozygous

231   positions and infer nuDNA haplotypes. Missing data can affect the success of haplotype

232   phasing and detection of identical sequences (Salerno *et al.*, 2015), therefore short sequence

233   reads were removed (*rag2*, *So. sechellensis*: Mahé = six, Praslin = two) and complete

234   alignments for all nuDNA loci constructed. Random four-digit seeds generated by the TRUE

235   RANDOM NUMBER SERVICE (Haahr, 2015) were applied to PHASE analyses which was run five

236   times per locus with the highest pseudo-likelihood score used to select the best-fit model of

237   haplotype estimation (Stephens & Donnelly, 2003). Heterozygous positions were deemed

238   those achieving a score ≥ 0.7 (Harrigan *et al.*, 2008) and coded according to the International

239   Union of Pure and Applied Chemistry. Remaining ambiguous positions were coded as 'N'. To

240   check for saturation across codon positions, the test of Xia (Xia *et al.*, 2003) was applied using

241   DAMBE v. 5.5.29 (Xia, 2013). To check for evidence of recombination, the DATAMONKEY

242   software suite (Pond & Frost, 2005; Delport *et al.*, 2010) was employed to select appropriate

243   models and run analyses using the GARD application (Kosakovsky Pond *et al.*, 2006a;

244   Kosakovsky Pond *et al.*, 2006b) under default settings. Haplotype networks were constructed

245   using TCS v. 1.21 (Clement *et al.*, 2000) with a 95% connection limit and gaps treated as a fifth

246   state. TCS networks were 'beautified' using TCSBU (Murias dos Santos *et al.*, 2016). Phased

247   sequence data was used to infer haplotypes.

248   To detect evidence of historical population expansion or contraction in *So.*

249   *sechellensis*, *So. thomasseti*, and *Se. gardineri* (*Se. pipilodryas* was excluded due to limited

250   sampling), we applied neutrality tests and performed skyline plots. Tajima's D (Tajima, 1989),

251   Fu's F_S (Fu, 1997), and the R_2 test statistic (Ramos-Onsins & Rozas, 2002) were run in DNASP

252   v. 5.10.1 (Librado & Rozas, 2009) and applied to each locus individually. One thousand

253   coalescent simulations were run for F_S and the R_2 test. A conventional P value of 0.05 was

254   adopted for Tajima's D and R_2; Fu's F_S is interpreted as significant at $P < 0.02$. We performed

255   Extended Bayesian Skyline plots (EBSP; Heled & Drummond, 2008) using unphased data for

256   each island-specific population in BEAST v. 2.4.8 via the CIPRES Science Gateway (Miller *et al*.,

257   2010). The Jeffrey's (1/x) prior was applied to the data but to reduce over-parameterisation

258   we adopted a strict clock and the HKY substitution model (Hasegawa *et al*., 1985) to locus-

259   specific partitions following the EBSP tutorial (http://www.beast2.org/tutorials). Chain length

260   ranged from 50 to 300 million generations, sampling every 10,000 generations. Convergence,

261   population size changes, and ESS values were assessed using TRACER, ESPB plots were

262   visualised using R (R CORE TEAM, 2017).

263   Finally, to investigate patterns suggestive of isolation by distance across all multi-

264   distributed sooglossid taxa, we performed Mantel tests with 999 permutations on

265   independent (to reduce conflict from incomplete sampling) *16s* and *cytb* matrices using the

266   VEGAN package (Oksanen *et al.*, 2017) in R (R CORE TEAM, 2017). The GEOGRAPHIC DISTANCE

267   MATRIX GENERATOR V. 1.2.3 (Ersts, 2012) was used to generate pairwise distance matrices

268   for geographic localities. Sequences without corresponding geographic data were omitted.

269   Sampling localities are shown in Fig. 1.

270

271   **RESULTS**

272   **Molecular phylogeny and genetic variation**

273   Our final mtDNA sequence alignment of 56 sooglossids (*So. thomasseti* = 9, *So sechellensis* =

274 37, *Se. gardineri* = 9, *Se. pipilodryas* = 1) contained corresponding sequence data totalling

275 1,080 sites for 51 individuals. We were unable to obtain *cytb* sequence data for five Silhouette

276 *Se. gardineri*, which constituted the majority (82%) of the total missing data of 3%. Rather

277 than omit Silhouette *Se. gardineri* from our analyses (we are unaware of alternative *cytb* data

278 for this taxon) we chose to maintain taxonomic coverage in all tree reconstructions.

279 Indels were present in the *16s* (*So. thomasseti* x1 double bp; *Se. gardineri* x2 single bp;

280 *Se pipilodryas* x3 single bp) and *pomc* (*Sechellophryne* spp. x1 triple bp) sequence profiles. No

281 evidence of saturation, or recombination events was detected in coding loci. Summary

282 statistics of informative, uninformative, variable, and constant sites are shown in Table 1.

283 Uncorrected and corrected genetic distances between taxa show values of 5.8%-14.0% and

284 6.1%-15.6% respectively (Table 2). Between population genetic distances are 2.0%-4.5%

285 (uncorrected) and 2.1%-4.7% (corrected) for *So. sechellensis*; 2.1% for *So. thomasseti*

286 (uncorrected and corrected); and 3.6% (uncorrected) and 3.7% (corrected) for *Se. gardineri*

287 (Table 3).

288 Our Bayesian and maximum likelihood mtDNA reconstructions displayed highly

289 concordant internal topologies (Fig. 2; Fig. S1.1), and recovered full support for the

290 monophyly of *Sooglossus* and *Sechellophryne*. Island-specific populations of *Se*. *gardineri* and

291 *So*. *thomasseti* are strongly supported. Geographic structuring in *So*. *sechellensis* receives

292 strong support in BI analysis but moderate support in the ML tree, recovering a sister

293 relationship between Mahé frogs and a clade comprising those from Silhouette and Praslin.

294 A further distinction between Silhouette and Praslin populations receives strong support.

295 Bayesian phylogenetic reconstructions applying the Yule tree prior reflect that of analyses

296 using the constant population tree prior but provide reduced support for the monophyly of

297 *Sooglossus* and independent island populations of *Se. gardineri* and *So. Sechellensis* (Fig.

298   S1.2).

299

Species trees and population boundaries

301   The multilocus species trees are broadly congruent with our mtDNA phylogenies (Fig. 2-3).

302   The single topological disparity being internal relationships of *So. sechellensis* whereby the

303   nuDNA species tree places Praslin frogs as sister to a clade comprised of those from Mahé

304   and Silhouette. This contrasts with the mtDNA phylogeny and species trees which place Mahé

305   frogs as sister to a Praslin and Silhouette clade. Clades and sub-clades are generally well

306   supported except in the nuDNA tree where *Sooglossus* and *Sechellophryne* receive moderate

307   support, and the sister taxon relationship between the Mahé and Silhouette populations of

308   *Se. gardineri* is unresolved.

309   Ten well-supported entities are indicated from bPTP analyses, eight of which

310   correspond with island populations of the multi-distributed sooglossid taxa shown in the

311   mtDNA phylogeny (Fig. 2; Table S1.5). The remaining two entities represent members of an

312   internal clade of *So. sechellensis* on Mahé; one a single sample from the southern-most

313   population, the other comprised of one sample from the southern-most population and one

314   from a more northerly locality (Fig. 1-2; Fig. S1.1-2; Table S1.5).

315

Nuclear DNA haplotypes

317   For each of the four nuclear loci, constructed networks show two or more high-frequency

318   haplotypes in combination with multiple species- and population-specific haplotypes (Fig. 4-

319   7). In the network for *pomc* (36 haplotypes; Fig. 4) two mutational steps separated both *So.*

320   *sechellensis* and *So. thomasseti*, and the Mahé and Silhouette populations of *Se. gardineri*.

321   One haplotype was shared between genera for *rag1* (37 haplotypes; Fig. 5) with seven

322　mutational steps separating *So. sechellensis* and *So. thomasseti*. The *rag2* network (123

323　haplotypes; Fig. 6) shows five mutational steps separating *So. sechellensis* and *So. thomasseti*,

324　and two mutational steps between one of the two *Se. pipilodryas* haplotypes and *Se.*

325　*gardineri*. No genus specific characters were observed for *rho* (26 haplotypes; Fig. 7) where

326　four haplotypes were shared between *Sooglossus* and *Sechellophryne*. Given the analytical

327　thresholds we set, three networks (*pomc*, *rag1*, *rag2*) were divergent enough to differentiate

328　(disconnect) genera and identify independent haplotypes for *Se. pipilodryas*. All loci displayed

329　unique island-specific haplotypes for each multi-distributed species.

330

331　**Population demography**

332　Neutrality tests to understand population demographics in the Sooglossidae showed mostly

333　negative values, indicating positive selection or recent population expansion (Table S1.6).

334　However, statistically significant negative values are observed only in calculations of F_S, which

335　may be less effective with small sample sizes (Ramos-Onsins & Rozas, 2002). Statistically

336　significant positive values are evident in *16s* for all three species for Tajima's *D* but not F_S.

337　Tajima's *D* is not as powerful as either F_S or the R_2 test statistic, and the R_2 test is considered

338　to be more effective when applied to smaller sample sizes (Ramos-Onsins & Rozas, 2002;

339　Ramirez-Soriano *et al.*, 2008). Significant positive values ($P < 0.05$) for a single locus in each

340　species (*cytb*: *Se. gardineri*; *rag2*: *So. sechellensis*; *pomc*: *So. thomasseti*) were returned for

341　the R_2 test. This suggests a lack of congruence that may be more indicative of differential

342　levels of ancestral polymorphisms, selective pressures, and substitution rates across species

343　and among loci, than statistically significant departures from neutrality.

344　　　In EBSP analyses the 95% highest posterior density (HPD) interval returned for Mahé

345　and Silhouette populations of *So. sechellensis*, *So. thomasseti* and *Se. gardineri* included 0,

346   therefore a constant population size for these taxa cannot be rejected (Table S1.7; Fig. S1.3-

347   5). However, recent (within the last ~20 k years) population expansion appears to have

348   occurred in *So. sechellensis* on Praslin (Fig. S1.3).

349

350   **Isolation by distance**

351   Matrices for our investigation of the effect of isolation by distance comprised 149 *So.*

352   *sechellensis*, 29 *So. thomasseti*, and 26 *Se. gardineri* for *16s*, and 39 *So. sechellensis* and 9 *So.*

353   *thomasseti* for *cytb*. Mantel tests indicated significant correlation between genetic and

354   geographic distances in all species for both loci (*16s*: *So. sechellensis*, $r = 0.8253$, $P < 0.001$;

355   *So. thomasseti*, $r = 0.9895$, $P < 0.001$; *Se gardineri*, $r = 0.9642$, $P < 0.001$; *cytb*: *So. sechellensis*,

356    $r = 0.6995$, $P < 0.001$; *So. thomasseti*, $r = 0.9755$, $P < 0.05$).

357

358   **DISCUSSION**

359   **Sooglossid phylogeny and genetic differentiation**

360   Our analyses provide the first multi-gene phylogeny to use island-specific sampling to reveal

361   intraspecific relationships within this endemic family. The mtDNA phylogeny supports our first

362   hypothesis—that cryptic sooglossid diversity exists across the three islands where these frogs

363   occur—and confirms the evolutionary distinctiveness of multiple geographically restricted

364   sooglossid populations (Fig. 2). Our second hypothesis—that cryptic diversity corresponds

365   with biogeographic (island) origin—is supported by independent evolutionary histories for

366   the multi-distributed *Sooglossus* and *Sechellophryne* spp. in the mtDNA phylogeny, with

367   distinct populations of *So. sechellensis* on Mahé, Silhouette, and Praslin, and *So. thomasseti*

368   and *Se. gardineri* on Mahé and Silhouette (Fig. 2).

369   Mean uncorrected genetic distances among taxa for *16s* clearly reflect the greater

370 differences expected between genera (range: 12.32%-14.04%; Table 2). Within genera, the

371 Jukes-Cantor (JC) corrected *p*-distances between *So. sechellensis* and *So. thomasseti* (6.1%),

372 and *Se. gardineri* and *Se. pipilodryas* (7.0%) exceed the values previously reported by van der

373 Meijden *et al*. (2007) (4.4% in *Sooglossus* and 5.7% in *Sechellophryne*) for sequence data of

374 comparable length. However, van der Meijden *et al*. (2007) sampled considerably fewer than

375 20 individuals in each case (*Sooglossus*: n = 7; *Sechellophryne*: n = 2); a limitation associated

376 with an increased probability of underestimation of nucleotide diversity (Luo *et al.*, 2015).

377 Estimations of genetic distance resulting from increased sampling are therefore more likely

378 to represent the true population mean (Luo *et al.*, 2015).

379 van der Meijden *et al*. (2007) also identified a JC corrected *p*-distance of 3.0% between

380 the Mahé and Silhouette populations of *So. thomasseti* but did so from four samples; two

381 from Mahé, two from Silhouette. We report a JC corrected *p*-distance of 2.1% from a pool of

382 29 individuals (Table 3) originating from four sites on the island of Mahé, and two sites on

383 Silhouette. The spatial representation of our sampling, and greater sample size is therefore

384 more likely to reflect a value closer to the true mean. Taylor *et al*. (2012) found uncorrected

385 *16s p*-distances of 4.1%-6.1% between the Mahé, Silhouette, and Praslin populations of *So.*

386 *sechellensis* from a total sample size of 26. We incorporate all but two of the *16s* sequences

387 arising from Taylor *et al*. (2012) (these two omissions are Praslin samples placed within the

388 Mahé clade in their study which are likely to be the result of laboratory contamination, as

389 subsequent *cytb* analysis reflects their geographic origin; J. Labisko, unpubl. data) and report

390 genetic distances of 2.1%-4.7% from 159 samples (Table 3).

391

392 **Species trees and population boundaries**

393 The multilocus species trees are highly congruent with our mtDNA phylogenies but clade

394   support differs between the mtDNA and nuDNA analyses (Fig. 3). The lower levels of support

395   displayed may reflect statistical inaccuracy from missing (*cytb*) sequence data as well as the

396   inherent differential qualities of the loci we sampled. While the specific status of *Sooglossus*

397   and *Sechellophryne* taxa are not in question, further exploration of the data incorporating

398   additional loci may elucidate the strength of relationship between the two isolated

399   populations of *Se. gardineri*. Overall, and in spite of topological disparity between two island

400   lineages of *So. sechellensis*, the multispecies coalescent and bPTP model independently

401   provide further support for the monophyly of multiple island-specific lineages of sooglossid

402   frogs. For *So. sechellensis*, bPTP results also indicate additional intraspecific structure within

403   the Mahé population.

404

405   **Nuclear variation**

406   There is an increasing body of evidence reporting discordant patterns between mtDNA and

407   nuDNA markers in animal systems (Toews & Brelsford, 2012). Discordance between

408   molecular markers may be especially pronounced in amphibians (Hoelzer, 1997; Monsen &

409   Blouin, 2003), and nuclear genes are frequently recognised for their conflicting results in

410   genealogical estimations in amphibian studies (e.g. Fisher-Reid & Wiens, 2011; Eto & Matsui,

411   2014). Our analyses identified multiple haplotypes shared between island populations,

412   species, and genera. Nevertheless, geographic structuring of the Sooglossidae is visibly

413   evident in the nuclear loci we sampled, showing numerous unique haplotypes across all multi-

414   distributed taxa and a commonality between our mtDNA and nuDNA datasets. While these

415   nuDNA patterns may indicate a level of diversity within each population that differentiates it

416   from congeners on other islands, the data are also likely to reflect incomplete sampling and

417   incomplete lineage sorting; the latter especially so considering maternal line of inheritance

418   and smaller effective population size of mtDNA in comparison to the diploid, bi-parental

419   nature of nuDNA.

420

421   **Biogeographic and conservation implications**

422   Due to their intolerance of salt water, trans-oceanic dispersal is assumed to be an infrequent

423   method of range expansion for amphibians (Duellman & Trueb, 1986; Green *et al.*, 1988; de

424   Queiroz, 2005). The presence of endemic amphibians on oceanic islands may therefore be

425   considered unusual, yet rafting is increasingly cited as an explanation for transoceanic

426   dispersal of frogs (Vences *et al.*, 2003; Heinicke *et al.*, 2007; Maddock *et al.*, 2014; Bell *et al.*,

427   2015a; Bell *et al.*, 2015b), and even caecilians (Measey *et al.*, 2006). However, in each case,

428   pioneering dispersers have mainland congeners. Aside from their sister taxon relationship

429   with the Nasikabatrachidae of India's Western Ghats, from which they may have diverged 66-

430   131 Ma—prior to the geographic separation of India and Seychelles (Biju & Bossuyt, 2003;

431   Roelants *et al.*, 2007; Ruane *et al.*, 2011; Pyron, 2014; Frazão *et al.*, 2015; Feng *et al.*, 2017)—

432   the Sooglossidae have no recent relatives. The level of evolutionary distinctiveness displayed

433   by these frogs, undoubtedly a result of their lengthy isolation, is clearly evidence of their

434   historic and continuing presence on the archipelago.

435   Following its separation from India, the inner Seychelles region has formed both a

436   continuous landmass of some 129,500 km^2, and been submerged to its present extent,

437   comprising an archipelago of 45 inner-islands covering ~247 km^2. Had the Seychelles Bank

438   ever been completely submerged, this would be strongly reflected in the composition of its

439   fauna and flora, with an expectation of greater similarity to that of Africa and/or Asia

440   (Nussbaum, 1984). The region has been subject to eustatic fluctuations, climatic variability,

441   and vicariant events, which have played an influential role in the distribution of its biota.

442   Recently identified phylogeographic patterns within the archipelago's endemic herpetofauna

443   have revealed a variety of geographic correlations: skinks and geckos broadly differentiate

444   into northern (Praslin and surrounding islands) and southern (Mahé, Silhouette, and

445   surrounding islands) groups (Rocha *et al.*, 2010; Rocha *et al.*, 2011; Rocha *et al.*, 2013; Valente

446   *et al.*, 2013; Rocha *et al.*, 2016a; Rocha *et al.*, 2016b); while for the non-sooglossid anurans, a

447   distinct lack of variability is shown in the multi-distributed treefrog *Tachycnemis seychellensis*

448   (Maddock *et al.*, 2014), conflicting with observed structuring in Seychelles endemic caecilians

449   (Adamson *et al.*, 2016; Maddock *et al.*, 2016; Maddock *et al.*, 2017). Our mtDNA analyses

450   appear to confirm the relationship posited by Taylor *et al*. (2012), namely that Silhouette and

451   Praslin populations of *So. sechellensis* comprise a clade sister to that of frogs from Mahé. Yet

452   our nuDNA species tree presents a topological contrast by inferring Praslin frogs as sister to a

453   Silhouette and Mahé clade; harmonious with the north-south split identified in other

454   Seychelles herpetofauna. This disparity raises the question as to what these conflicting

455   biogeographic patterns in the data may reflect.

456   Since the Late Pleistocene, regional instability caused by either hydro-isostatic uplift

457   of the Seychelles Bank or volcanic subsidence (Montaggioni & Hoang, 1988) and substantial

458   low sea-level stands (Colonna *et al.*, 1996; Camoin *et al.*, 2004) have likely generated irregular

459   cycles of biogeographic isolation and reconnection across the Seychelles. Bathymetric data

460   indicate a sea-level drop of ~60 m bpsl would effectively link the granitic islands (Rocha *et al.*,

461   2013; Ali, 2018), providing the opportunity for dispersal and connection/reconnection of

462   previously disparate populations. Incongruence between and among the phylogeographic

463   patterns exhibited by Seychelles' herpetofauna are undoubtedly the result of a number of

464   contributory factors, including the inherent ecology and dispersal ability of each taxon.

465   Although these and other aspects are yet to be fully explored, Maddock *et al*. (2014) found

466 low levels of genetic variation in *T. seychellensis* concluding, *inter-alia*, that relatively recent

467 admixture during low sea-level stands may explain this observation. The treefrogs are

468 regularly encountered in appropriate habitat at lower elevations down to sea-level, and may

469 on occasion raft across the ocean as a means of dispersal, as their ancestors are believed to

470 have done from Madagascar (Vences *et al.*, 2003; Maddock *et al.*, 2014). The terrestrial

471 Sooglossidae (although *Sechellophryne* spp. may be observed in low-level vegetation; Gerlach

472 & Willi, 2002; J. Labisko, pers. obs.) are generally restricted to high elevation moist forest,

473 such that lower (and dryer) elevations combined with even a limited oceanic distance

474 between suitable habitats, may act as a considerable barrier to dispersal. However, the

475 islands of Mahé and Silhouette share high elevation peaks, similar forest habitat, and are

476 currently separated by less than 20 km, and given a significant drop in sea level, the

477 opportunity for dispersal between the two would inevitably increase. Mahé and Silhouette

478 frogs may therefore be expected to share greater similarities than either do with those from

479 Praslin—an island which is lower, drier, 37 km distant from Mahé, and 51 km from

480 Silhouette—and the locus-specific nuDNA gene trees produced in our multispecies coalescent

481 analyses display a largely congruent topology, suggesting these loci are representative of true

482 relationships across the nuclear genome.

483   Clear geographic patterns of discordance between mtDNA and nuDNA are likely to

484 exclude incomplete lineage sorting as an underlying explanation, and may instead indicate

485 biogeographic discordance (Funk & Omland, 2003; Toews & Brelsford, 2012). Extended

486 periods of isolation combined with previous range contact are an intrinsic factor in most taxa

487 that display patterns of this nature, during which high frequency mutations accumulate and

488 are followed by interbreeding in hybrid zones upon range reconnection, generating divergent

489 patterns in the mtDNA and nuDNA genomes (Toews & Brelsford, 2012). The cycles of

490   emergence and submergence of the Seychelles Bank are unknown but the patterns of genetic

491   differentiation and population demography we report could be attributed to infrequent

492   stable environmental conditions of adequate duration that would arise as a result of

493   significant but sporadic eustatic fluctuations, and should not be discounted as a mechanism

494   to explain the patterns observed in our data. It is noteworthy that one population—*So.*

495   *sechellensis* from Praslin—appears to have recently expanded (Fig. S1.3). That no other

496   sooglossids are found on Praslin suggests that (i) *So. sechellensis* is the only sooglossid to have

497   occurred here, or (ii) other members of the Sooglossidae have since died out, perhaps as a

498   result of the climactic effects and loss of terrestrial habitat following deglaciation and the rise

499   in sea levels from the Late Pleistocene to Early Holocene (Dutton *et al*., 2015; Woodroffe *et*

500   *al*., 2015). In either scenario, the Praslin frogs have seemingly been successful in exploiting

501   available habitat on this island in the absence of other sooglossids.

502   Reciprocal monophyly in mtDNA together with significant divergence in nuDNA loci

503   have long been criteria for defining evolutionarily significant units (Moritz, 1994). Our results

504   meet these criteria, showing numerous unique, geographically specific haplotypes in nuclear

505   loci, and reciprocal monophyly in mtDNA for sooglossid populations, additional analyses of

506   which indicates significant effects of isolation by distance. Sooglossid lineages that reflect

507   island origin are defined across all multi-distributed species: *So. sechellensis* on Mahé,

508   Silhouette, and Praslin, and *So. thomasseti* and *Se. gardineri* on Mahé and Silhouette (Fig. 2-

509   3). Furthermore, and in accordance with the criteria ascribed by Vieites *et al*. (2009), we

510   consider these lineages as unconfirmed candidate species. Given the limitations of species

511   delimitation methods in distinguishing structure from population isolation versus species

512   boundaries (Sukumaran & Knowles, 2017; Leaché *et al*., 2018) (evidenced in our study by the

513   identification of intraspecific structure within the Mahé population of *So. sechellensis*; Fig. 2;

514 Table S1.5), a continuing formal taxonomic appraisal for the Sooglossidae, combining multiple

515 lines of evidence to corroborate hypotheses of distinct lineages is underway and will be

516 presented elsewhere.

517 Our investigation of an understudied insular taxon, endemic to the Seychelles

518 archipelago, adds to the developing biogeographic picture of this unique region. Patterns of

519 cryptic diversity in Seychelles' amphibians have only recently begun to be explored, yet

520 already appear to be highly prevalent and complex. Prior to our study, four sooglossid species

521 were recognised across the three islands upon which they occur, with one population—the

522 only sooglossid found on the island of Praslin, *So. sechellensis*—determined as fitting the

523 criteria of an additional ESU (Taylor *et al.*, 2012). The cryptic diversity we have uncovered

524 denotes a total of eight independent island lineages that should be managed accordingly.

525 Such management action should include regular long-term population and habitat

526 assessments, support of the genetic integrity of each ESU by carrying out no inter-island

527 translocations, and the establishment of regular screening activities for invasive pathogens

528 including *Batrachochytrium dendrobatidis*, *B. salamandrivorans*, and *Ranavirus*—notably, the

529 Seychelles is one of only two global regions where pathogenic chytrid is yet to be detected

530 (Labisko *et al*, 2015; Lips, 2016). The identification of distinct, island-specific populations of

531 these frogs warrants continued investigation of their intraspecific relationships, and further

532 insights are likely to reveal additional factors important for their future conservation.

533

553 **REFERENCES**

554 **Adamson EAS, Saha A, Maddock ST, Nussbaum RA, Gower DJ, Streicher JW. 2016.**

555   Microsatellite discovery in an insular amphibian (*Grandisonia alternans*) with

556   comments on cross-species utility and the accuracy of locus identification from

557   unassembled Illumina data. *Conservation Genetics Resources* **8:** 541-551.

558 **Adsersen H. 1995.** Research on islands: Classic, recent, and prospective approaches. In:

559   Vitousek PM, Loope LL and Adsersen H, eds. *Islands*. Berlin, Heidelberg: Springer Berlin

560   Heidelberg. 7-21.

561 **Ali JR. 2017.** Islands as biological substrates: classification of the biological assemblage

562   components and the physical island types. *Journal of Biogeography* **44:** 984-994.

563 **Ali JR. 2018.** Islands as biological substrates: Continental. *Journal of Biogeography* **45:** 1003-

564   1018.

565 **Alonso R, Crawford AJ, Bermingham E. 2012.** Molecular phylogeny of an endemic radiation

566   of Cuban toads (Bufonidae: *Peltophryne*) based on mitochondrial and nuclear genes.

567   *Journal of Biogeography* **39:** 434-451.

568 **Bell RC, Drewes RC, Channing A, Gvoždík V, Kielgast J, Lötters S, Stuart BL, Zamudio KR,**

569   **Emerson B. 2015a.** Overseas dispersal of *Hyperolius* reed frogs from Central Africa to

570   the oceanic islands of São Tomé and Príncipe. *Journal of Biogeography* **42:** 65-75.

571 **Bell RC, Drewes RC, Zamudio KR. 2015b.** Reed frog diversification in the Gulf of Guinea:

572   overseas dispersal, the progression rule, and in situ speciation. *Evolution* **69:** 904-915.

573 **Biju SD, Bossuyt F. 2003.** New frog family from India reveals an ancient biogeographical link

574   with the Seychelles. *Nature* **425:** 711-714.

575 **Boettger O. 1896.** Neue Kriechthiere (Scelotes, *Arthroleptis*) von den Seychellen. *Zoologischer*

576   *Anzeiger* **19:** 349.

577 **Bouckaert R, Heled J, Kuhnert D, Vaughan T, Wu CH, Xie D, Suchard MA, Rambaut A,**

578 **Drummond AJ. 2014.** BEAST 2: a software platform for Bayesian evolutionary analysis.

579 *PLoS Computational Biology* **10:** e1003537.

580 **Boulenger GA. 1909.** No. XVI.-A list of the freshwater fishes, batrachians, and reptiles

581 obtained by Mr. J. Stanley Gardiner's expedition to the Indian Ocean. *Transactions of*

582 *the Linnean Society of London. 2nd Series: Zoology* **12:** 291-300.

583 **Boulenger GA. 1911.** No. XVII.-List of the batrachians and reptiles obtained by Prof. Stanley

584 Gardiner on his second expedition to the Seychelles and Aldabra. *Transactions of the*

585 *Linnean Society of London. 2nd Series: Zoology* **14:** 375-378.

586 **Camoin GF, Montaggioni LF, Braithwaite CJR. 2004.** Late glacial to post glacial sea levels in

587 the western Indian Ocean. *Marine Geology* **206:** 119-146.

588 **Castresana J. 2000.** Selection of conserved blocks from multiple alignments for their use in

589 phylogenetic analysis. *Molecular Biology and Evolution* **17:** 540-552.

590 **Chatterjee S, Goswami A, Scotese CR. 2013.** The longest voyage: Tectonic, magmatic, and

591 paleoclimatic evolution of the Indian plate during its northward flight from Gondwana

592 to Asia. *Gondwana Research* **23:** 238-267.

593 **Clement M, Posada D, Crandall KA. 2000.** TCS: a computer program to estimate gene

594 genealogies. *Molecular Ecology* **9:** 1657-1659.

595 **Collier JS, Sansom V, Ishizuka O, Taylor RN, Minshull TA, Whitmarsh RB. 2008.** Age of

596 Seychelles–India break-up. *Earth and Planetary Science Letters* **272:** 264-277.

597 **Colonna M, Casanova J, Dullo W-C, Camoin G. 1996.** Sea-level changes and $\delta18O$ record for

598 the past 34,000 yr from Mayotte Reef, Indian Ocean. *Quaternary Research* **46:** 335-

599 339.

600 **Cronk QCB. 1997.** Islands: stability, diversity, conservation. *Biodiversity and Conservation* **6:**

601   477-493.

602   **Darwin C. 1859.** *On the origin of species*. Murray: London.

603   **Davies D, Francis TJG. 1964.** The crustal structure of the Seychelles bank. *Deep Sea Research*

604   *and Oceanographic Abstracts* **11:** 921-927.

605   **de Queiroz A. 2005.** The resurrection of oceanic dispersal in historical biogeography. *Trends*

606   *in Ecology and Evolution* **20:** 68-73.

607   **Delport W, Poon AF, Frost SD, Kosakovsky Pond SL. 2010.** Datamonkey 2010: a suite of

608   phylogenetic analysis tools for evolutionary biology. *Bioinformatics* **26:** 2455-2457.

609   **Drummond AJ, Ho SY, Phillips MJ, Rambaut A. 2006.** Relaxed phylogenetics and dating with

610   confidence. *PLoS Biology* **4:** e88.

611   **Drummond AJ, Rambaut A. 2007.** BEAST: Bayesian evolutionary analysis by sampling trees.

612   *BMC Evolutionary Biology* **7:** 214.

613   **Duellman WE, Trueb L. 1986.** *Biology of amphibians*. Johns Hopkins University Press.

614   **Dutton A, Webster JM, Zwartz D, Lambeck K, Wohlfarth B. 2015.** Tropical tales of polar ice:

615   evidence of Last Interglacial polar ice sheet retreat recorded by fossil reefs of the

616   granitic Seychelles islands. *Quaternary Science Reviews* **107:** 182-196.

617   **Dyer M, Sailsbery J, McClellan D. n.d.** DataConvert–biological data file conversion. Available

618   at   http://www.mybiosoftware.com/dataconvert-1-0-converts-proteindna-data-

619   formats.html

620   **Edgar RC. 2004.** MUSCLE: multiple sequence alignment with high accuracy and high

621   throughput. *Nucleic Acids Research* **32:** 1792-1797.

622   **Ersts P. 2012.** Geographic Distance Matrix Generator version 1.23: American Museum of

623   Natural History.

624   **Eto K, Matsui M. 2014.** Cytonuclear discordance and historical demography of two brown

625   frogs, *Rana tagoi* and *R. sakuraii* (Amphibia: Ranidae). *Molecular Phylogenetics and*

626   *Evolution* **79:** 231-239.

627   **Felsenstein J. 1981.** Evolutionary trees from DNA sequences: a maximum likelihood approach.

628   *Journal of Molecular Evolution* **17:** 368-376.

629   **Feng YJ, Blackburn DC, Liang D, Hillis DM, Wake DB, Cannatella DC, Zhang P. 2017.**

630   Phylogenomics reveals rapid, simultaneous diversification of three major clades of

631   Gondwanan frogs at the Cretaceous-Paleogene boundary. *Proceedings of the National*

632   *Academy of Sciences of the United States of America* **114:** E5864-E5870.

633   **Fisher-Reid MC, Wiens J. 2011.** What are the consequences of combining nuclear and

634   mitochondrial data for phylogenetic analysis? Lessons from *Plethodon* salamanders

635   and 13 other vertebrate clades. *BMC Evolutionary Biology* **11:** 300.

636   **Frazão A, da Silva HR, Russo CA. 2015.** The Gondwana breakup and the history of the Atlantic

637   and Indian Oceans unveils two new clades for early neobatrachian diversification. *PLoS*

638   *One* **10:** e0143926.

639   **Frost DR, Grant T, Faivovich J, Bain RH, Haas A, Haddad CFB, De Sá RO, Channing A,**

640   **Wilkinson M, Donnellan SC, Raxworthy CJ, Campbell JA, Blotto BL, Moler P, Drewes**

641   **RC, Nussbaum RA, Lynch JD, Green DM, Wheeler WC. 2006.** The Amphibian Tree of

642   Life. *Bulletin of the American Museum of Natural History* **297:** 1-291.

643   **Fu YX. 1997.** Statistical tests of neutrality of mutations against population growth, hitchhiking

644   and background selection. *Genetics* **147:** 915-925.

645   **Funk DJ, Omland KE. 2003.** Species-level paraphyly and polyphyly: Frequency, causes, and

646   consequences, with insights from animal mitochondrial DNA. *Annual Review of*

647   *Ecology, Evolution, and Systematics* **34:** 397-423.

648   **Gene Codes Corporation. 2015.** Sequencher® version 5.3 sequence analysis software. Ann

649   Arbor, MI USA.

650   **Gerlach J, Willi J. 2002.** A new species of frog, genus *Sooglossus* (Anura, Sooglossidae) from

651   Silhouette Island, Seychelles. *Amphibia-Reptilia* **23:** 445-458.

652   **Gissi C, San Mauro D, Pesole G, Zardoya R. 2006.** Mitochondrial phylogeny of Anura

653   (Amphibia): a case study of congruent phylogenetic reconstruction using amino acid

654   and nucleotide characters. *Gene* **366:** 228-237.

655   **Glez-Pena D, Gomez-Blanco D, Reboiro-Jato M, Fdez-Riverola F, Posada D. 2010.** ALTER:

656   program-oriented conversion of DNA and protein alignments. *Nucleic Acids Research*

657   **38:** W14-18.

658   **Green DM, Nussbaum RA, Datong Y. 1988.** Genetic divergence and heterozygosity among

659   frogs of the family Sooglossidae. *Herpetologica* **44:** 113-119.

660   **Haahr M. 2015.** True Random Number Service: http://www.random.org.

661   **Harrigan RJ, Mazza ME, Sorenson MD. 2008.** Computation vs. cloning: evaluation of two

662   methods for haplotype determination. *Molecular Ecology Resources* **8:** 1239-1248.

663   **Hasegawa M, Kishino H, Yano T. 1985.** Dating of the human-ape splitting by a molecular clock

664   of mitochondrial DNA. *Journal of Molecular Evolution* **22:** 160-174.

665   **Heinicke MP, Duellman WE, Hedges SB. 2007.** Major Caribbean and Central American frog

666   faunas originated by ancient oceanic dispersal. *Proceedings of the National Academy*

667   *of Sciences of the United States of America* **104:** 10092-10097.

668   **Heled J, Drummond AJ. 2008.** Bayesian inference of population size history from multiple loci.

669   *BMC Evolutionary Biology* **8:** 289.

670   **Heled J, Drummond AJ. 2010.** Bayesian inference of species trees from multilocus data.

671   *Molecular Biology and Evolution* **27:** 570-580.

672   **Hoelzer GA. 1997.** Inferring phylogenies from mtDNA variation: mitochondrial-gene trees

673   versus nuclear-gene trees revisited. *Evolution* **51:** 622-626.

674   **Huelsenbeck JP, Ronquist F, Nielsen R, Bollback JP. 2001.** Bayesian inference of phylogeny

675   and its impact on evolutionary biology. *Science* **294:** 2310-2314.

676   **Irisarri I, San Mauro D, Green DM, Zardoya R. 2010.** The complete mitochondrial genome of

677   the relict frog *Leiopelma archeyi*: insights into the root of the frog Tree of Life.

678   *Mitochondrial DNA* **21:** 173-182.

679   **Isaac NJ, Redding DW, Meredith HM, Safi K. 2012.** Phylogenetically-informed priorities for

680   amphibian conservation. *PLoS One* **7:** e43912.

681   **IUCN SSC Amphibian Specialist Group. 2013a.** *Sechellophryne gardineri The IUCN Red List of*

682   *Threatened Species 2013*.

683   **IUCN SSC Amphibian Specialist Group. 2013b.** *Sechellophryne pipilodryas The IUCN Red List*

684   *of Threatened Species 2013*.

685   **IUCN SSC Amphibian Specialist Group. 2013c.** *Sooglossus sechellensis The IUCN Red List of*

686   *Threatened Species 2013*.

687   **IUCN SSC Amphibian Specialist Group. 2013d.** *Sooglossus thomasseti The IUCN Red List of*

688   *Threatened Species 2013*.

689   **Jockusch EL, Martínez-Solano I, Timpe EK. 2015.** The effects of inference method, population

690   sampling, and gene sampling on species tree inferences: An empirical study in slender

691   salamanders (Plethodontidae: Batrachoseps). *Systematic Biology* **64:** 66-83.

692   **Kosakovsky Pond SL, Posada D, Gravenor MB, Woelk CH, Frost SD. 2006a.** Automated

693   phylogenetic detection of recombination using a genetic algorithm. *Molecular Biology*

694   *and Evolution* **23:** 1891-1901.

695   **Kosakovsky Pond SL, Posada D, Gravenor MB, Woelk CH, Frost SD. 2006b.** GARD: a genetic

696   algorithm for recombination detection. *Bioinformatics* **22:** 3096-3098.

697 **Labisko J, Maddock ST, Taylor ML, Chong-Seng L, Gower DJ, Wynne FJ, Wombwell E, Morel**

698 **C, French GCA, Bunbury N, Bradfield KS. 2015.** Chytrid fungus (*Batrachochytrium*

699 *dendrobatidis*) undetected in the two orders of Seychelles amphibians. *Herpetological*

700 *Review* **46:** 41-45.

701 **Lambert SM, Reeder TW, Wiens JJ. 2015.** When do species-tree and concatenated estimates

702 disagree? An empirical analysis with higher-level scincid lizard phylogeny. *Molecular*

703 *Phylogenetics and Evolution* **82 Pt A:** 146-155.

704 **Lanfear R, Calcott B, Ho SY, Guindon S. 2012.** Partitionfinder: combined selection of

705 partitioning schemes and substitution models for phylogenetic analyses. *Molecular*

706 *Biology and Evolution* **29:** 1695-1701.

707 **Leaché AD, Zhu T, Rannala B, Yang Z. 2018.** The spectre of too many species. *Systematic*

708 *Biology*.

709 **Lepage T, Bryant D, Philippe H, Lartillot N. 2007.** A general comparison of relaxed molecular

710 clock models. *Molecular Biology and Evolution* **24:** 2669-2680.

711 **Librado P, Rozas J. 2009.** DnaSP v5: a software for comprehensive analysis of DNA

712 polymorphism data. *Bioinformatics* **25:** 1451-1452.

713 **Lips KR. 2016.** Overview of chytrid emergence and impacts on amphibians. *Philosophical*

714 *transactions of the Royal Society of London. Series B, Biological sciences* **371**.

715 **Los Alamos National Security LLC. 2005-2006.** Format Converter: U.S. Department of Energy's

716 National   Nuclear   Security   Administration:

717 https://www.hiv.lanl.gov/content/sequence/FORMAT_CONVERSION/form.html

718 **Luo A, Lan H, Ling C, Zhang A, Shi L, Ho SY, Zhu C. 2015.** A simulation study of sample size for

719 DNA barcoding. *Ecology and Evolution* **5:** 5869-5879.

720 **MacArthur RH, Wilson EO. 1967.** *Theory of island biogeography*. Princeton University Press:

721   Princeton.

722   **Maddock ST, Briscoe AG, Wilkinson M, Waeschenbach A, San Mauro D, Day JJ, Littlewood**

723   **DT, Foster PG, Nussbaum RA, Gower DJ. 2016.** Next-generation mitogenomics: A

724   comparison of approaches applied to caecilian amphibian phylogeny. *PLoS One* **11:**

725   e0156757.

726   **Maddock ST, Day JJ, Nussbaum RA, Wilkinson M, Gower DJ. 2014.** Evolutionary origins and

727   genetic variation of the Seychelles treefrog, *Tachycnemis seychellensis* (Dumeril and

728   Bibron, 1841) (Amphibia: Anura: Hyperoliidae). *Molecular Phylogenetics and Evolution*

729   **75:** 194-201.

730   **Maddock ST, Wilkinson M, Nussbaum RA, Gower DJ. 2017.** A new species of small and highly

731   abbreviated caecilian (Gymnophiona: Indotyphlidae) from the Seychelles island of

732   Praslin, and a recharacterization of *Hypogeophis brevis* Boulenger, 1911. *Zootaxa*

733   **4329:** 301.

734   **Maia-Carvalho B, Goncalves H, Ferrand N, Martinez-Solano I. 2014.** Multilocus assessment

735   of phylogenetic relationships in *Alytes* (Anura, Alytidae). *Molecular Phylogenetics and*

736   *Evolution* **79:** 270-278.

737   **Matthews DH, Davies D. 1966.** Geophysical studies of the Seychelles Bank. *Philosophical*

738   *Transactions of the Royal Society A: Mathematical, Physical and Engineering Sciences*

739   **259:** 227-239.

740   **Measey GJ, Vences M, Drewes RC, Chiari Y, Melo M, Bourles B. 2006.** Freshwater paths

741   across the ocean: molecular phylogeny of the frog *Ptychadena newtoni* gives insights

742   into amphibian colonization of oceanic islands. *Journal of Biogeography* **34:** 7-20.

743   **Miller MA, Pfeiffer W, Schwartz T. 2010.** Proceedings of the Gateway Computing

744   Environments Workshop (GCE) *Creating the CIPRES science gateway for inference of*

745   *large phylogenetic trees*: IEEE New Orleans. 1-8.

746   **Monsen KJ, Blouin MS. 2003.** Genetic structure in a montane ranid frog: restricted gene flow

747   and nuclear-mitochondrial discordance. *Molecular Ecology* **12:** 3275-3286.

748   **Montaggioni LF, Hoang CT. 1988.** The last interglacial high sea level in the granitic Seychelles,

749   Indian ocean. *Palaeogeography, Palaeoclimatology, Palaeoecology* **64:** 79-91.

750   **Moritz C. 1994.** Defining 'Evolutionarily Significant Units' for conservation. *Trends in Ecology*

751   *and Evolution* **9:** 373-375.

752   **Murias dos Santos A, Cabezas MP, Tavares AI, Xavier R, Branco M. 2016.** tcsBU: a tool to

753   extend TCS network layout and visualization. *Bioinformatics* **32:** 627-628.

754   **Noble GK. 1931.** *The biology of the Amphibia*. McGraw-Hill Book Company, Inc.: New York

755   and London.

756   **Nussbaum RA. 1984.** Amphibians of the Seychelles. In: Stoddart DR, ed. *Biogeography and*

757   *ecology of the Seychelles Islands*. The Hague; Boston: Hingham, Massachusetts, USA:

758   W. Junk. 379-415.

759   **Oksanen J, Blanchet FG, Friendly M, Kindt R, Legendre P, McGlinn D, Minchin PR, O'Hara RB,**

760   **Simpson GL, Solymos P, M. Henry H. Stevens, Szoecs E, Wagner H. 2017.** vegan:

761   Community Ecology Package. 2.4-4. ed.

762   **Paulay G. 1994.** Biodiversity on oceanic Islands: Its origin and extinction. *American Zoologist*

763   **34:** 134-144.

764   **Pond SL, Frost SD. 2005.** Datamonkey: rapid detection of selective pressure on individual sites

765   of codon alignments. *Bioinformatics* **21:** 2531-2533.

766   **Pyron RA. 2014.** Biogeographic analysis reveals ancient continental vicariance and recent

767   oceanic dispersal in amphibians. *Systematic Biology* **63:** 779-797.

768   **Pyron RA, Wiens JJ. 2011.** A large-scale phylogeny of Amphibia including over 2800 species,

769 and a revised classification of extant frogs, salamanders, and caecilians. *Molecular*

770 *Phylogenetics and Evolution* **61:** 543-583.

771 **R Core Team. 2017.** R: A language and environment for statistical computing. Vienna, Austria.:

772 R Foundation for Statistical Computing.

773 **Rambaut A. 2016.** FigTree 1.4.3.

774 **Rambaut A, Suchard MA, Xie D, Drummond AJ. 2014.** Tracer v1.6.

775 **Ramirez-Soriano A, Ramos-Onsins SE, Rozas J, Calafell F, Navarro A. 2008.** Statistical power

776 analysis of neutrality tests under demographic expansions, contractions and

777 bottlenecks with recombination. *Genetics* **179:** 555-567.

778 **Ramos-Onsins SE, Rozas J. 2002.** Statistical properties of new neutrality tests against

779 population growth. *Molecular Biology and Evolution* **19:** 2092-2100.

780 **Robertson JM, Langin KM, Sillett TS, Morrison SA, Ghalambor CK, Funk WC. 2014.** Identifying

781 evolutionarily significant units and prioritizing populations for management on

782 islands. *Monographs of the Western North American Naturalist* **7:** 397-411.

783 **Rocha S, Harris D, Posada D. 2011.** Cryptic diversity within the endemic prehensile-tailed

784 gecko *Urocotyledon inexpectata* across the Seychelles Islands: patterns of

785 phylogeographical structure and isolation at the multilocus level. *Biological Journal of*

786 *the Linnean Society* **104:** 177-191.

787 **Rocha S, Harris DJ, Carretero M. 2010.** Genetic diversity and phylogenetic relationships of

788 *Mabuya* spp. (Squamata: Scincidae) from western Indian Ocean islands. *Amphibia-*

789 *Reptilia* **31:** 375-385.

790 **Rocha S, Perera A, Bunbury N, Kaiser-Bunbury CN, Harris DJ. 2016a.** Speciation history and

791 species-delimitation within the Seychelles Bronze geckos, *Ailuronyx* spp.: molecular

792 and morphological evidence. *Biological Journal of the Linnean Society*.

793 **Rocha S, Perera A, Silva A, Posada D, Harris DJ. 2016b.** Evolutionary history of *Trachylepis*

794   skinks in the Seychelles islands: introgressive hybridization, morphological evolution

795   and geographic structure. *Biological Journal of the Linnean Society* **119:** 15-36.

796 **Rocha S, Posada D, Harris DJ. 2013.** Phylogeography and diversification history of the day-

797   gecko genus *Phelsuma* in the Seychelles islands. *BMC Evolutionary Biology* **13:** 3.

798 **Roelants K, Gower DJ, Wilkinson M, Loader SP, Biju SD, Guillaume K, Moriau L, Bossuyt F.**

799   **2007.** Global patterns of diversification in the history of modern amphibians.

800   *Proceedings of the National Academy of Sciences of the United States of America* **104:**

801   887-892.

802 **Ruane S, Pyron RA, Burbrink FT. 2011.** Phylogenetic relationships of the Cretaceous frog

803   *Beelzebufo* from Madagascar and the placement of fossil constraints based on

804   temporal and phylogenetic evidence. *Journal of Evolutionary Biology* **24:** 274-285.

805 **Salerno PE, Senaris JC, Rojas-Runjaic FJ, Cannatella DC. 2015.** Recent evolutionary history of

806   Lost World endemics: population genetics, species delimitation, and phylogeography

807   of sky-island treefrogs. *Molecular Phylogenetics and Evolution* **82 Pt A:** 314-323.

808 **Santos AMC, Field R, Ricklefs RE. 2016.** New directions in island biogeography. *Global Ecology*

809   *and Biogeography* **25:** 751-768.

810 **Silvestro D, Michalak I. 2012.** raxmlGUI: a graphical front-end for RAxML. *Organisms Diversity*

811   *& Evolution* **12:** 335-337.

812 **Stamatakis A. 2014.** RAxML version 8: a tool for phylogenetic analysis and post-analysis of

813   large phylogenies. *Bioinformatics* **30:** 1312-1313.

814 **Stephens M, Donnelly P. 2003.** A comparison of bayesian methods for haplotype

815   reconstruction from population genotype data. *American Journal of Human Genetics*

816   **73:** 1162-1169.

817 **Stephens M, Scheet P. 2005.** Accounting for decay of linkage disequilibrium in haplotype

818 inference and missing-data imputation. *American Journal of Human Genetics* **76:** 449-

819 462.

820 **Stephens M, Smith NJ, Donnelly P. 2001.** A new statistical method for haplotype

821 reconstruction from population data. *American Journal of Human Genetics* **68:** 978-

822 989.

823 **Sukumaran J, Knowles LL. 2017.** Multispecies coalescent delimits structure, not species.

824 *Proceedings of the National Academy of Sciences* **114:** 1607-1612.

825 **Tajima F. 1989.** Statistical method for testing the neutral mutation hypothesis by DNA

826 polymorphism. *Genetics* **123:** 585-595.

827 **Talavera G, Castresana J. 2007.** Improvement of phylogenies after removing divergent and

828 ambiguously aligned blocks from protein sequence alignments. *Systematic Biology* **56:**

829 564-577.

830 **Tamura K, Stecher G, Peterson D, Filipski A, Kumar S. 2013.** MEGA6: Molecular Evolutionary

831 Genetics Analysis version 6.0. *Molecular Biology and Evolution* **30:** 2725-2729.

832 **Taylor ML, Bunbury N, Chong-Seng L, Doak N, Kundu S, Griffiths RA, Groombridge JJ. 2012.**

833 Evidence for evolutionary distinctiveness of a newly discovered population of

834 sooglossid frogs on Praslin Island, Seychelles. *Conservation Genetics* **13:** 557-566.

835 **Toews DP, Brelsford A. 2012.** The biogeography of mitochondrial and nuclear discordance in

836 animals. *Molecular Ecology* **21:** 3907-3930.

837 **Vaidya G, Lohman DJ, Meier R. 2011.** SequenceMatrix: concatenation software for the fast

838 assembly of multi-gene datasets with character set and codon information. *Cladistics*

839 **27:** 171-180.

840 **Valente J, Rocha S, Harris DJ. 2013.** Differentiation within the endemic burrowing skink

841   *Pamelaescincus gardineri*, across the Seychelles islands, assessed by mitochondrial

842   and nuclear markers. *African Journal of Herpetology* **63:** 25-33.

843 **van der Meijden A, Boistel R, Gerlach J, Ohler A, Vences M, Meyer A. 2007.** Molecular

844   phylogenetic evidence for paraphyly of the genus *Sooglossus*, with the description of

845   a new genus of Seychellean frogs. *Biological Journal of the Linnean Society* **91:** 347 -

846   359.

847 **Vences M, Vieites DR, Glaw F, Brinkmann H, Kosuch J, Veith M, Meyer A. 2003.** Multiple

848   overseas dispersal in amphibians. *Proceedings of the Royal Society B: Biological*

849   *Sciences* **270:** 2435-2442.

850 **Vieites DR, Wollenberg KC, Andreone F, Kohler J, Glaw F, Vences M. 2009.** Vast

851   underestimation of Madagascar's biodiversity evidenced by an integrative amphibian

852   inventory. *Proceedings of the National Academy of Sciences of the United States of*

853   *America* **106:** 8267-8272.

854 **Wallace AR. 1869.** *The Malay Archipelago: the land of the orang-utan and the bird of paradise;*

855   *a narrative of travel, with studies of man and nature*. Courier Corporation.

856 **Warren BH, Simberloff D, Ricklefs RE, Aguilee R, Condamine FL, Gravel D, Morlon H,**

857   **Mouquet N, Rosindell J, Casquet J, Conti E, Cornuault J, Fernandez-Palacios JM,**

858   **Hengl T, Norder SJ, Rijsdijk KF, Sanmartin I, Strasberg D, Triantis KA, Valente LM,**

859   **Whittaker RJ, Gillespie RG, Emerson BC, Thebaud C. 2015.** Islands as model systems

860   in ecology and evolution: prospects fifty years after MacArthur-Wilson. *Ecology*

861   *Letters* **18:** 200-217.

862 **Whittaker RJ, Fernández-Palacios JM. 2007.** *Island biogeography: Ecology, evolution, and*

863   *conservation*. OUP Oxford.

864 **Woodroffe SA, Long AJ, Milne GA, Bryant CL, Thomas AL. 2015.** New constraints on late

865   Holocene eustatic sea-level changes from Mahé, Seychelles. *Quaternary Science*

866   *Reviews* **115:** 1-16.

867   **Xia X. 2013.** DAMBE5: a comprehensive software package for data analysis in molecular

868   biology and evolution. *Molecular Biology and Evolution* **30:** 1720-1728.

869   **Xia X, Xie Z, Salemi M, Chen L, Wang Y. 2003.** An index of substitution saturation and its

870   application. *Molecular Phylogenetics and Evolution* **26:** 1-7.

871   **Zhang J, Kapli P, Pavlidis P, Stamatakis A. 2013.** A general species delimitation method with

872   applications to phylogenetic placements. *Bioinformatics* **29:** 2869-2876.

873   **Zoological   Society   of   London.   2015.**   EDGE   of   Existence   Programme.

874   https://www.edgeofexistence.org/species/species-category/amphibians/   Accessed

875   14th October 2018.

876   **Table 1** Sequenced gene fragments and summary statistics for analysed loci from *Sooglossus*

877   and *Sechellophryne* spp. tissue samples. Mitochondrial DNA = *16S* rRNA (*16s*), cytochrome b

878   (*cytb*); nuclear DNA = proopiomelanocortin (*pomc*), recombination activating genes (*rag*) 1

879   and 2, rhodopsin exon 1 (*rho*). Data incorporates *16s* sequence data obtained from GenBank

880   (superscript denotes no. of GenBank samples included in total). Dash (-) indicates sequence

881   data not obtained. *N*=sample size; bp=base pairs; Pi=parsimony informative sites; V=variable

882   sites; π=nucleotide diversity.

Species	Island	*16s*	*cytb*	*pomc*	*rag1*	*rag2*	*rho*
So. sechellensis	Mahé	76[6]	16	10	19	59	18
	Silhouette	21	12	9	15	20	13
	Praslin	62[15]	11	11	25	51	19
So. thomasseti	Mahé	17	7	6	11	15	7
	Silhouette	12	2	2	10	12	2
Se. gardineri	Mahé	15	4	7	10	15	11
	Silhouette	12	-	1	3	10	3
Se. pipilodryas	Silhouette	2[1]	1	1	1[1]	2[1]	1
	N	217	53	47	94	184	74
	bp	532	549	348	383	521	279
	Pi	111	154	31	22	57	13
	V	119	184	42	32	76	15
	π	0.0557	0.1113	0.0312	0.0169	0.0232	0.0043

Table 2 Between taxa *16s* distance matrix for the Sooglossidae. Lower diagonal: uncorrected *p*-distance; upper diagonal: corrected Jukes-Cantor *p*-distance (Jukes & Cantor, 1969). *Sechellophryne gardineri* = Sg; *Se. pipilodryas* = Sp; *Sooglossus sechellensis* = Ss; *So. thomasseti* = St.

	Sg	Sp	Ss	St
Sg		0.0704	0.1435	0.1346
Sp	0.0672		0.1555	0.1447
Ss	0.1306	0.1404		0.0608
St	0.1232	0.1316	0.0584	

Table 3 Between population *16s p*-distance distance matrix for the Sooglossidae. Lower diagonal: uncorrected *p*-distance; upper diagonal: corrected Jukes-Cantor *p*-distance (Jukes & Cantor, 1969). *Sechellophryne gardineri* = Sg; *Se. pipilodryas* = Sp; *Sooglossus sechellensis* = Ss; *So. thomasseti* = St. M = Mahé, S = Silhouette, P = Praslin.

|	Sg-M	Sg-S	Sp	Ss-M	Ss-P	Ss-S	St-M	St-S
Sg-M		0.0373	0.0701	0.1491	0.1477	0.1479	0.1407	0.1243
Sg-S	0.0364		0.0708	0.1395	0.1339	0.1402	0.1383	0.1313
Sp	0.0669	0.0675		0.1546	0.1551	0.1599	0.1473	0.1410
Ss-M	0.1352	0.1273	0.1397		0.0465	0.0399	0.0577	0.0622
Ss-P	0.1341	0.1226	0.1401	0.0451		0.0205	0.0647	0.0623
Ss-S	0.1342	0.1279	0.1440	0.0389	0.0202		0.0556	0.0572
St-M	0.1283	0.1263	0.1337	0.0556	0.0620	0.0536		0.0209
St-S	0.1145	0.1205	0.1285	0.0597	0.0598	0.0551	0.0206	
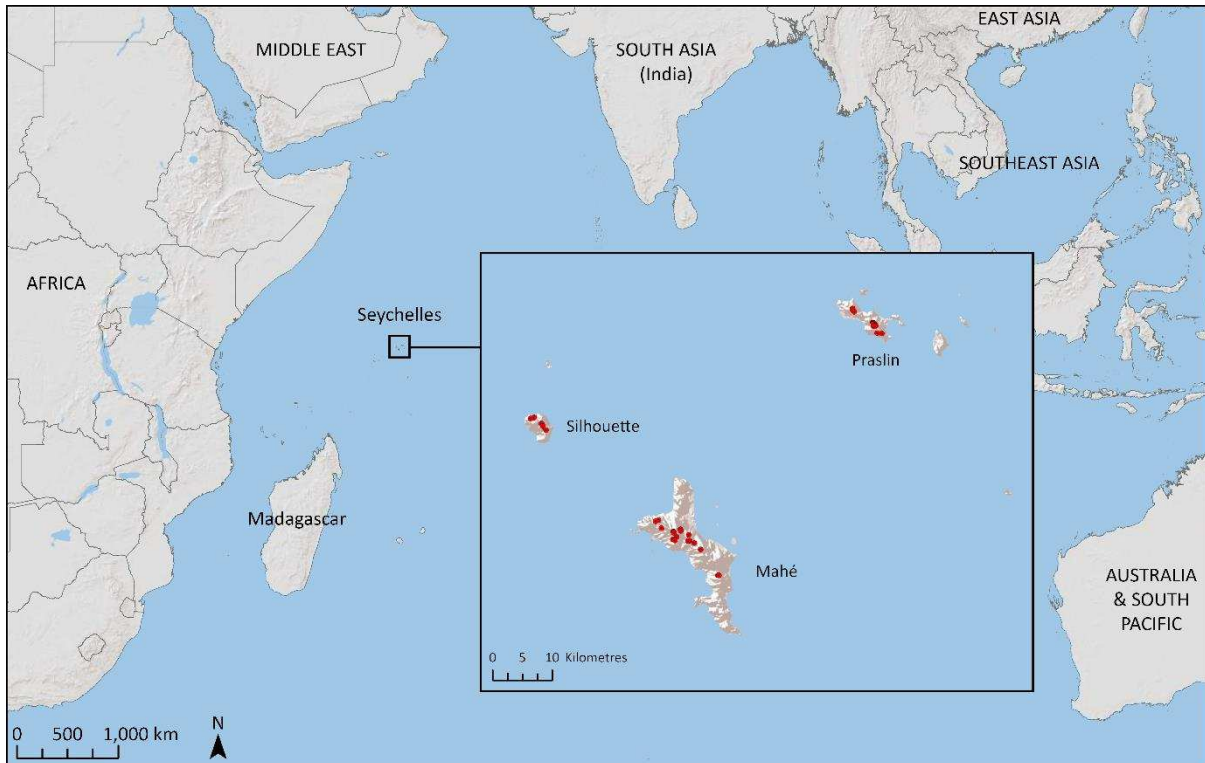
 Figure 1 Seychelles archipelago and the surrounding geographic regions of the Indian Ocean, inset with the inner islands of Mahé, Praslin, and Silhouette—the only locations where the Sooglossidae (Noble, 1931) are found. *Sooglossus sechellensis* (Boettger, 1896), *So. thomasseti* (Boulenger, 1909), and *Sechellophryne gardineri* (Boulenger, 1911) are sympatric on Mahé and Silhouette, with the addition of *Se. pipilodryas* (Gerlach & Willi, 2002) on Silhouette. *Sooglossus sechellensis* is the only sooglossid to occur on Praslin. Red circles indicate sampling localities and associated geographic data used to test for the effects of isolation by distance.
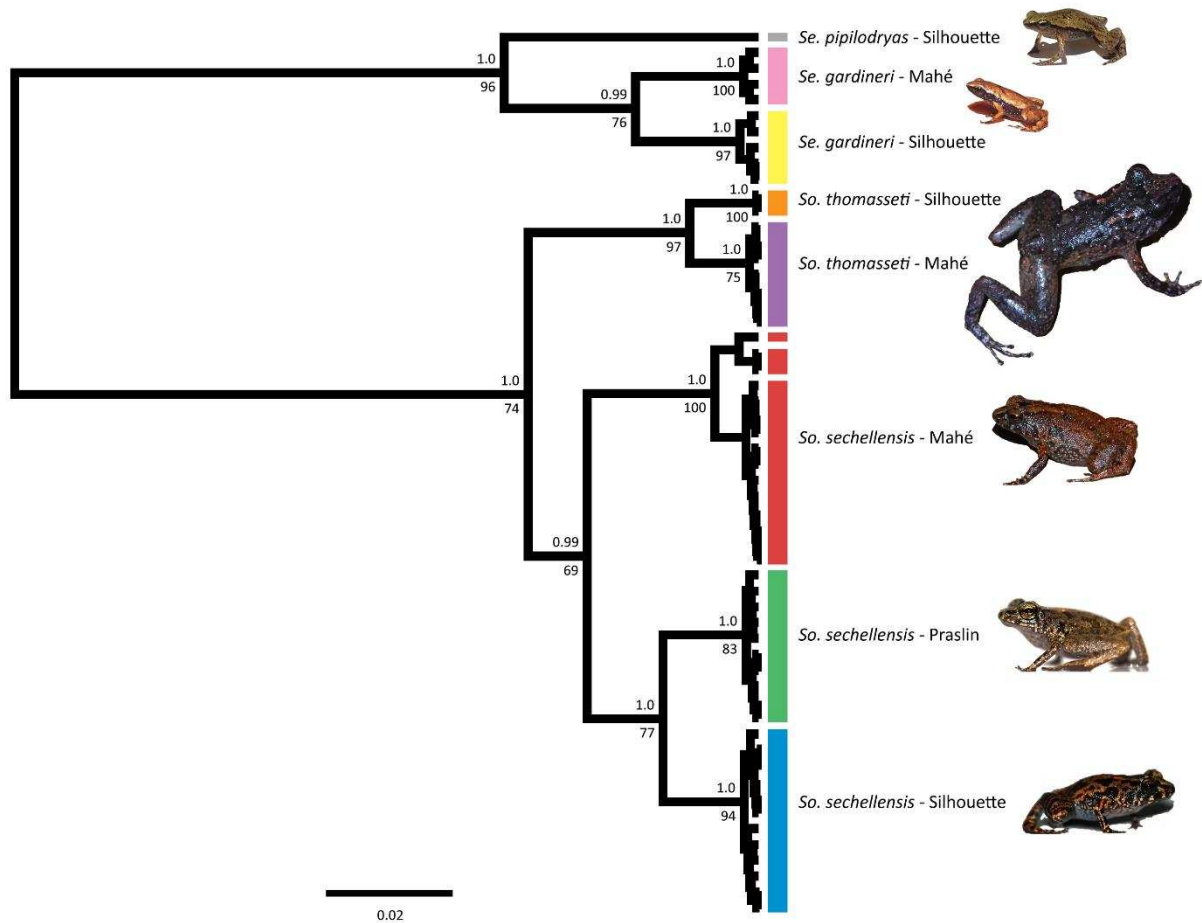
Figure 2 Bayesian inferred mitochondrial DNA phylogeny of Seychelles Sooglossidae. Support values are shown as Bayesian posterior probabilities (PP: above branches) and maximum likelihood bootstrap values (BS: below branches). Scale bar indicates substitutions per site. Vertical coloured bars adjacent to branch tips correspond to the ten population/species boundaries returned by the maximum likelihood partition in bPTP analysis. Colour coding identifies the island lineage of each species: *Sooglossus thomasseti* (Mahé – orange; Silhouette – purple) is the largest sooglossid; followed by *So. sechellensis* (Mahé – red; Praslin – green; Silhouette – blue), which is also the most widely geographically distributed; then *Sechellophryne pipilodryas* (Silhouette – grey); and the smallest in the family, *Sechellophryne gardineri* (Mahé – pink; Silhouette – yellow).
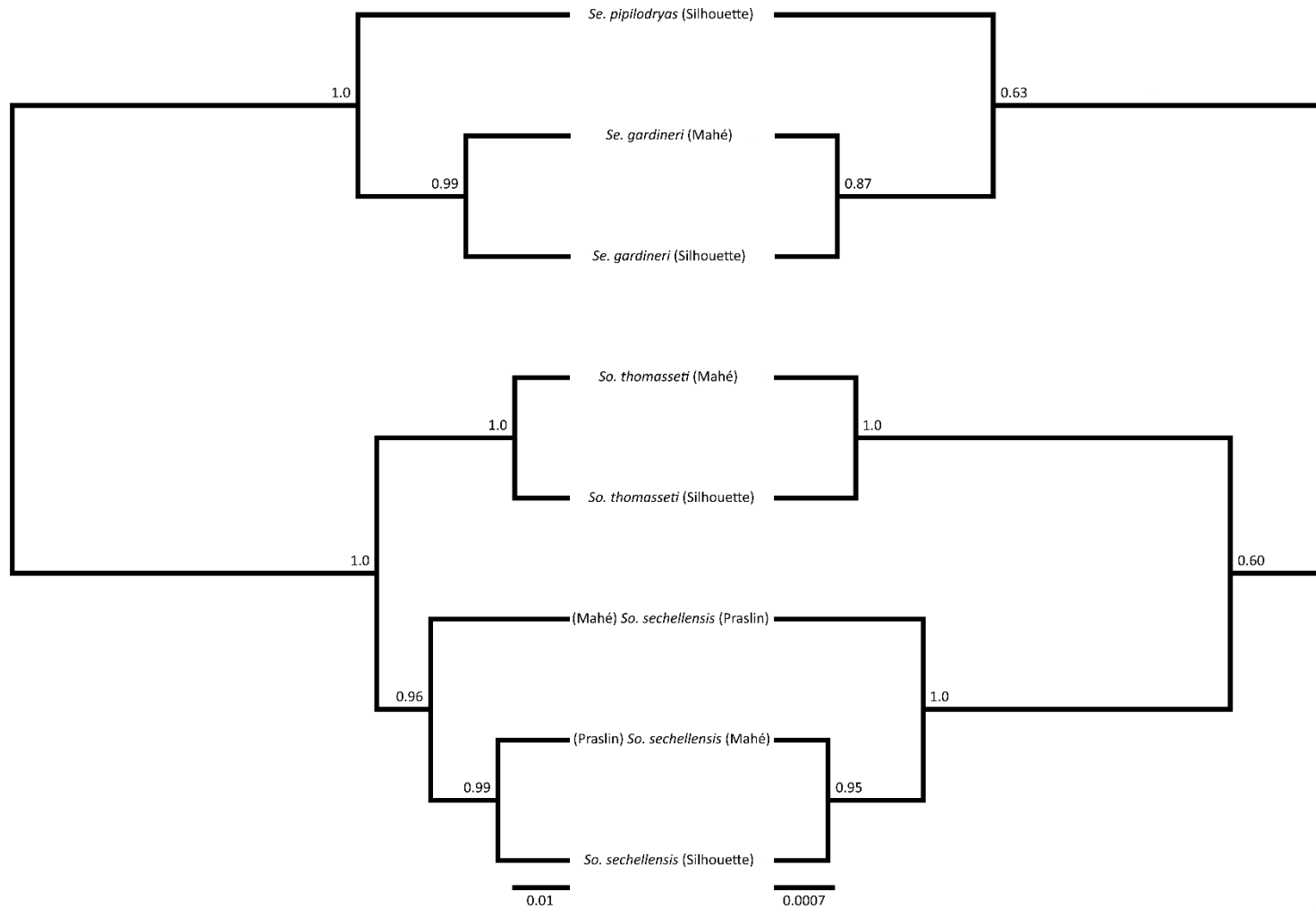
Figure 3 *BEAST generated mitochondrial (left) and nuclear (right) DNA species trees for the Sooglossidae. Branch numbers show PP support. The single topological disparity identifies Mahé *So. sechellensis* in the mtDNA species tree as sister to a clade comprised of those from Silhouette and Praslin, whereas in the nuDNA tree Silhouette and Mahé frogs form a clade sister to those from Praslin. Scale bar indicates substitutions per site.
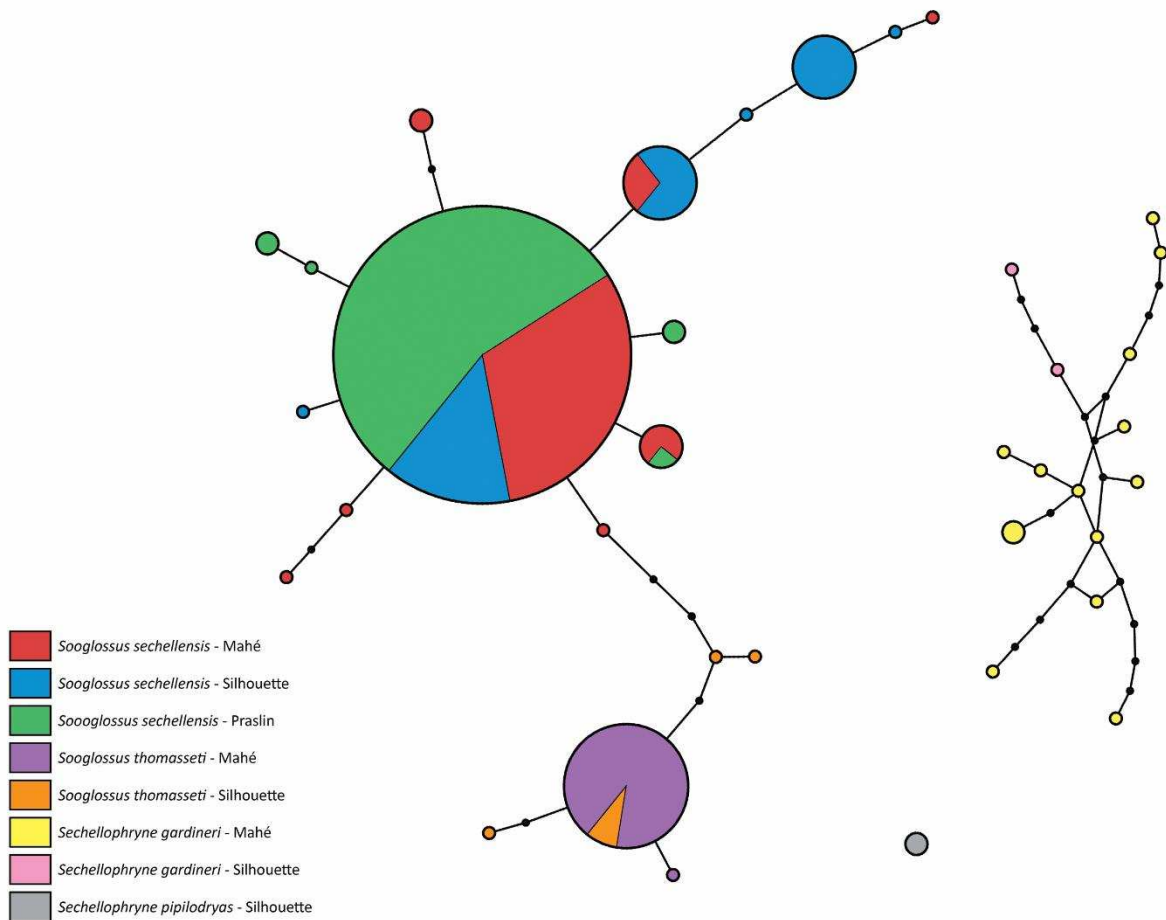
Figure 4 Nuclear *pomc* DNA haplotype network for the Sooglossidae. Thirty-six haplotypes are present. Circle size is proportional to the frequency with which the haplotype was observed, i.e. larger circles represent high-frequency, shared haplotypes, smaller circles represent low-frequency/rare haplotypes. Closed black circles indicate mutational steps. Colours represent island populations (see legend/Fig. 2).
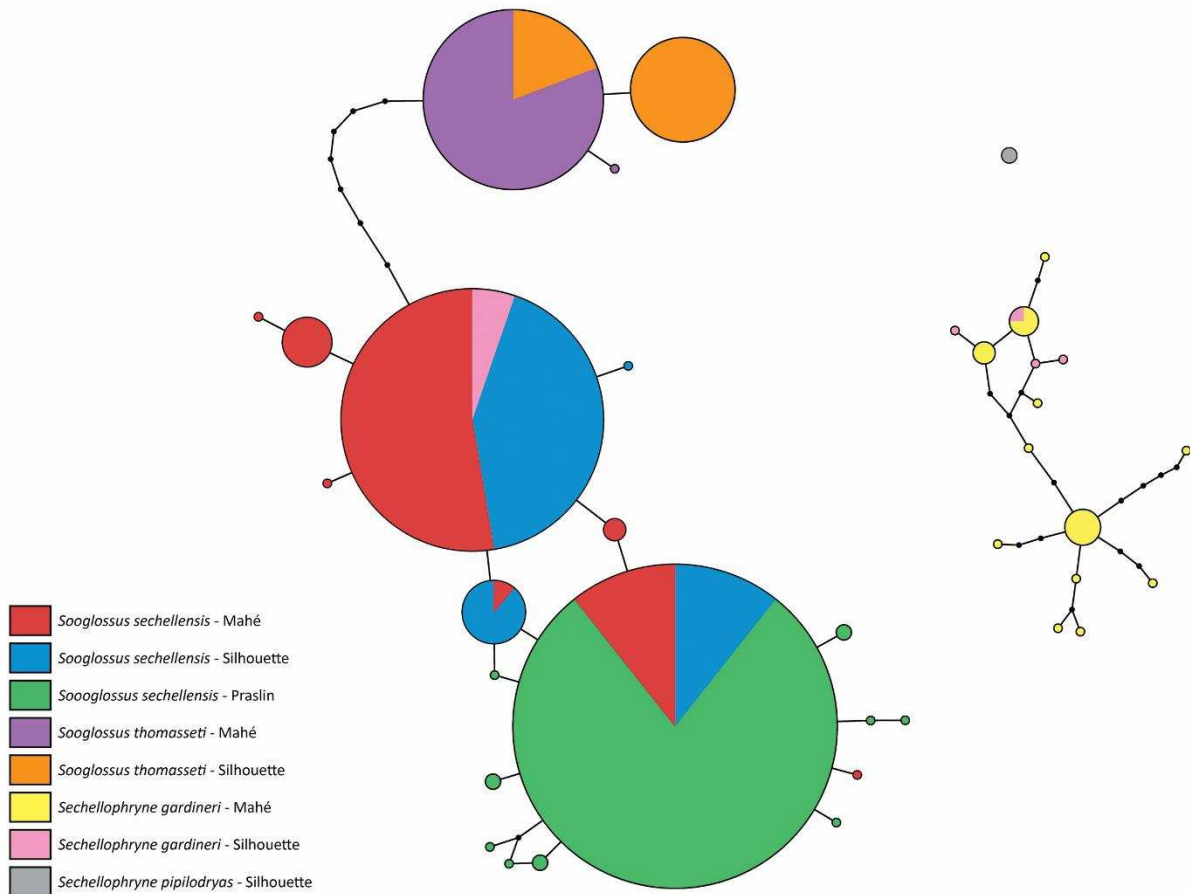
Figure 5 Nuclear *rag1* DNA haplotype network for the Sooglossidae. Thirty-seven haplotypes are present. Circle size is proportional to the frequency with which the haplotype was observed, i.e. larger circles represent high-frequency, shared haplotypes, smaller circles represent low-frequency/rare haplotypes. Closed black circles indicate mutational steps. Colours represent island populations; colour coding follows that of previous figures.

Figure 6 Nuclear *rag2* DNA haplotype network for the Sooglossidae. One-hundred and twenty-three haplotypes are present. Circle size is proportional to the frequency with which the haplotype was observed, i.e. larger circles represent high-frequency, shared haplotypes, smaller circles represent low-frequency/rare haplotypes. Closed black circles indicate mutational steps. Colours represent island populations; colour coding follows that of previous figures.
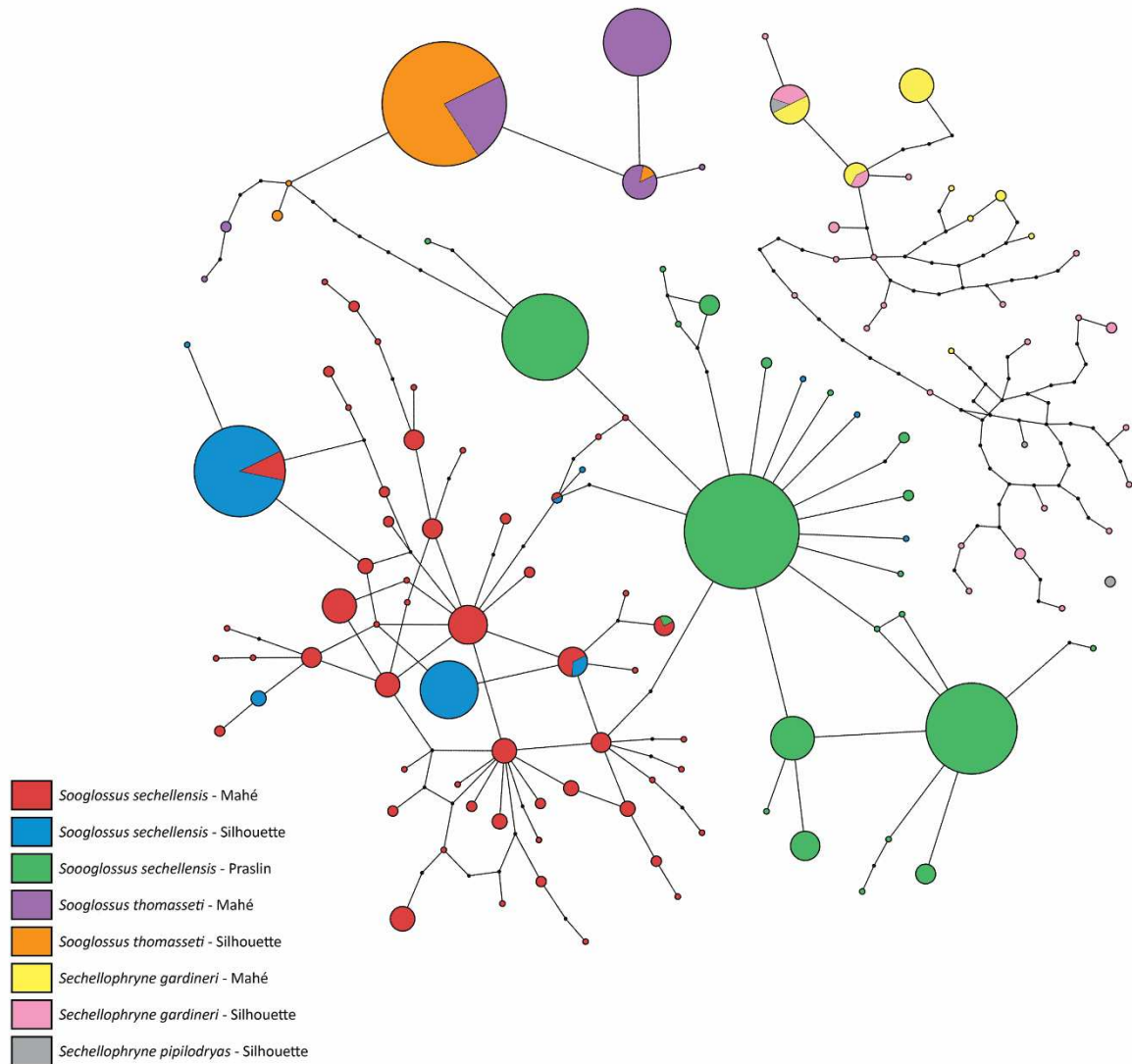
Figure 7 Nuclear *rho* DNA haplotype network for the Sooglossidae. Twenty-six haplotypes are present. Circle size is proportional to the frequency with which the haplotype was observed, i.e. larger circles represent high-frequency, shared haplotypes, smaller circles represent low-frequency/rare haplotypes. Closed black circles indicate mutational steps. Colours represent island populations; colour coding follows that of previous figures.
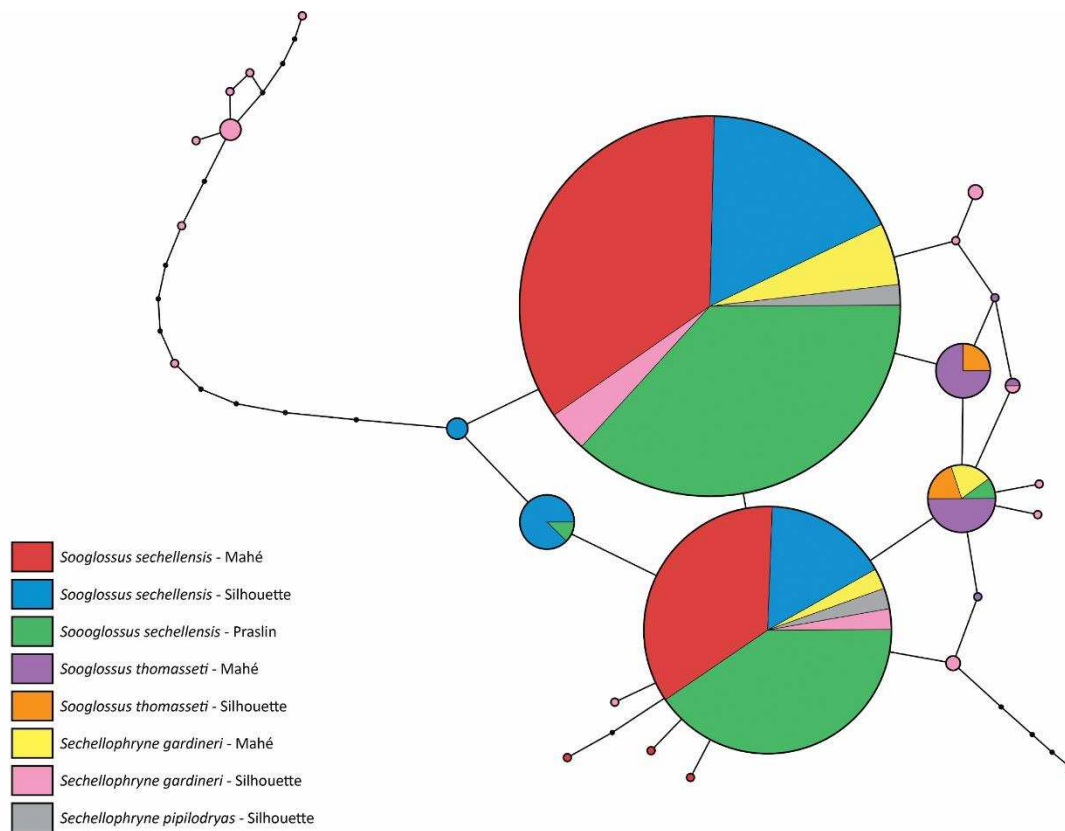
SUPPORTING INFORMATION

Appendix S1

PCR cycling conditions & sequence data

Sequences from two mitochondrial (mtDNA) and four nuclear (nuDNA) loci were amplified via standard polymerase-chain reaction (PCR) with total reaction volumes of 10-42 µl. Due to difficulty obtaining adequate DNA yields from such small biological samples (toe-clips from frogs regularly less than 10 mm SVL) volumes of template DNA varied between some reactions. For a 25 µl reaction, reaction volumes consisted of 10.5 µl ddH$_2$O, 0.5 µl each of forward and reverse primer (at a concentration of 25 pmol/µl), 12.5 µl MyTaq HS Red mix™, and 1 µl of template DNA. Details of primers used are shown in Table S1. Primer pairs developed for this study were generated using Primer-Blast (https://www.ncbi.nlm.nih.gov/tools/primer-blast). PCR cycling conditions were: denature at 95°C for 60 seconds (*16s*, *cytb*, *rag2*) or 94°C for 60 seconds (*pomc*, *rag1*, *rho*); followed by 35 (*16s*, *cytb*, *rag2*, *rho*) or 40 (*rag1*, *pomc*) cycles of denaturing at 95°C for 15 seconds (*16s*, *cytb*, *rag2*), or 94°C for 30 seconds (*pomc*, *rag1*, *rho*); annealing for 15 seconds at 53°C (*16s*, *cytb*), 59.5°C (*rag2*), or for 30 seconds at 56°C (*rag1*), 57°C (*pomc*), 60°C (*rho*); extending at 72°C for 10 seconds (*16s*, *cytb*), or 30 seconds (*pomc*, *rag1*, *rag2*, *rho*), with a final extension step of 72°C for 5 minutes. All *16s* samples were sequenced in both directions. Due to project constraints complimentary sequence data were not generated for all loci. Those obtained comprised the following: *cytb* = 17; *pomc* = 9; *rag1* = 2; *rag2* = 8; *rho* = 4. All sequences were cross-checked using the BLAST function in MEGA6 (Tamura, Stecher, Peterson, Filipski, & Kumar, 2013) and compared against sequences generated by this study. Ambiguous bases were coded accordingly.

Table S1.1 Primers used for PCR amplification and sequencing.

Gene fragment	Primer	Sequence (5' – 3')
16s	*16s* A-L[a]	CGC CTG TTT ATC AAA AAC AT
	16s B-H[a]	CCG GTC TGA ACT CAG ATC ACG T
cytb	CBJ 10933[b]	TAT GTT CTA CCA TGA GGA CAA ATA TC
	Cytb-c[b]	CTA CTG GTT GTC CTC CGA TTC ATG T
	CytbJL1f[c]	TAG ACC TCC CAA CCC CAT CC
	CytbJL1r[c]	GAG GTG TGT GTT AGT GGG GG
	CytbSGJL1f[c]	ACC GCT TTC GTA GGC TAT GT
	CytbSGJL1[c]	GTG GAC GAA ATG ATA TTG CTC GT
pomc	POMCJLf[c]	GAC ATC GCC AAC TAT CCG GT
	POMCJLr[c]	AAG TGT TGT CCC CCG TGT TT
	POMCJL2f[c]	AAA CAC GGG GGA CAA CAC TT
	POMCJL2r[c]	CTT CTG AGT CGA CAC CAG GG
rag1	RAG1B[d]	ATG GGA GAT GTG AGT GAR AAR CA
	RAG1E[d]	TCC GCT GCA TTT CCR ATG TCR CA
rag2	RAG2 JG1-F[c]	TCG TCC TAC CAT GTT CAC CAA TGA GT
	RAG2 JG1-R[c]	TCC TGT CCA ATC AGG CAG TTC CA
	RAG2JLSG1f[c]	CCA GCA GTG ACC AGC ATC TT
	RAG2JLSG1r[c]	CGC TGT CTC TTG GAC TGG TT
	RAG2JLSG2r[c]	CCG ACA ATG AGG AAC TCG CT
rho	Rhod1A[e]	ACC ATG AAC GGA ACA GAA GGY CC
	Rhod1D[e]	GTA GCG AAG AAR CCT TCA AMG TA

[a] Palumbi *et al*., (1991)
[b] Chiari *et al*., (2004)
[c] Developed for this study
[d] Biju & Bossuyt, (2003)
[e] Bossuyt & Milinkovitch, (2000)

Table S1.2 GenBank derived sequence data used in this study. Codes indicate Genbank accession numbers. Identical codes in adjacent columns for *Ascaphus truei* and *Leiopelma archeyi* represent sampling of independent sections of the mitochondrial genome of the same accessioned data.

Species	*16s*	*cytb*	*rag1*	*rag2*
Ascaphus truei	AJ871087	AJ871087	-	-
Leiopelma archeyi	NC_014691	NC_014691	-	-
Sechellophryne pipilodryas	DQ872918	-	DQ872922	DQ872912
Sooglossus sechellensis	JF784361	-	-	-
Sooglossus sechellensis	JF784362	-	-	-
Sooglossus sechellensis	JF784363	-	-	-
Sooglossus sechellensis	JF784364	-	-	-
Sooglossus sechellensis	JF784365	-	-	-
Sooglossus sechellensis	JF784366	-	-	-
Sooglossus sechellensis	JF784367	-	-	-
Sooglossus sechellensis	JF784368	-	-	-
Sooglossus sechellensis	JF784370	-	-	-
Sooglossus sechellensis	JF784371	-	-	-
Sooglossus sechellensis	JF784372	-	-	-
Sooglossus sechellensis	JF784373	-	-	-
Sooglossus sechellensis	JF784374	-	-	-
Sooglossus sechellensis	JF784376	-	-	-
Sooglossus sechellensis	JF784377	-	-	-
Sooglossus sechellensis	JF784378	-	-	-
Sooglossus sechellensis	JF784379	-	-	-
Sooglossus sechellensis	JF784380	-	-	-
Sooglossus sechellensis	JF784381	-	-	-
Sooglossus sechellensis	JF784382	-	-	-
Sooglossus sechellensis	JF784383	-	-	-

Table S1.3 Partitioning schemes and substitution models selected by PartitionFinder v1.1.1 (Lanfear *et al.*, 2012) using the AIC criterion for Bayesian (BEAST2/*BEAST) analyses. Codon positions in parentheses.

	Partitioning scheme	**Substitution model**
mtDNA	*16s, cytb* (1)	GTR+I+G
	cytb (2)	TrN+I
	cytb (3)	TrN+G
nuDNA	*pomc* (1-3)	TrN+I+G
	rag1 (1-3)	TrN+I+G
	rag2 (1-3)	TrN+I+G
	rho (1-3)	TrN+I+G

Table S1.4 Taxa used as composites in *BEAST analyses.

Species	Ref.	Locus	Composite
Sechellophryne gardineri	JMSG07	*rho*	JMSG09
Sechellophryne pipilodryas	DQ872922	*rag1*	JMSP01

Table S1.5 Species/population boundaries inferred from Bayesian Poisson Tree Processes (bPTP) analysis. The BEAST2 mtDNA phylogeny was used as the input tree. Posterior probabilities (PP) of maximum likelihood and Bayesian analyses were identical. Populations are listed in node order as per the phylogeny (Fig. 2 in the main text).

Species/population	Island	Sample reference	PP
Sechellophryne pipilodryas	Silhouette	JMSP01	1.00
Sechellophryne gardineri	Mahé	CDSG01, MBSG04, LRSG03, MBSG02	0.97
Sechellophryne gardineri	Silhouette	DGSG01, JMSG01, JMSG05, JMSG07, JMSG10	0.75
Sooglossus thomasseti	Silhouette	GBST01, JMST06	0.99
Sooglossus thomasseti	Mahé	CDST02, CRST01, MCST02, LMST01, MSST01, CDST01, MBST01	0.98
Sooglossus sechellensis	Mahé	LRSS14	0.95
Sooglossus sechellensis	Mahé	LRSS01, MSSS02	0.95
Sooglossus sechellensis	Mahé	RSS01, LRSS02, LMSS01, SFSS02, CRSS14, CSS01, MSSS01, MCSS10, MBSS07, CRSS02, CRSS01, MBSS01	0.97
Sooglossus sechellensis	Praslin	VMSP16, CMSP01, CMSP07, CMSP02, FPSP03, FAT2, ZSP01, ZSP04, ZSP03, ZSP08	0.98
Sooglossus sechellensis	Silhouette	JMSS05, GBSS01, JMSS11, JMSS08, GBSS07, JMSS01, JMSS04, JMSS03, JMSS07, GBSS10, JMSS06, JMSS09	0.98

Table S1.6 Population demographic tests for the Sooglossidae. Positive values of Tajima's D and Fu's F_S indicate stable population structure, balancing selection or recent population decrease; negative values indicate positive selection, or suggest evidence of recent population expansion. Tajima's D and R_2 are interpreted as significant at $P < 0.05$, Fu's F_S at $P < 0.02$.

	Sooglossus sechellensis			*Sooglossus thomasseti*			*Sechellophryne gardineri*		
	Tajima's D	Fu's F_S	R_2	Tajima's D	Fu's F_S	R_2	Tajima's D	Fu's F_S	R_2
16s	2.36870	3.278	0.1621	3.10581	12.422	0.2512	2.24857	3.284	0.2073
	$P < 0.05$	$P > 0.02$	$P > 0.05$	$P < 0.01$	$P > 0.02$	$P > 0.05$	$P < 0.05$	$P > 0.02$	$P > 0.05$
cytb	1.71837	-1.421	0.1910	0.44661	3.394	0.1967	-0.55827	-0.361	0.1061
	$P > 0.05$	$P > 0.02$	$P > 0.05$	$P > 0.05$	$P > 0.02$	$P > 0.05$	$P > 0.05$	$P > 0.02$	$P < 0.05$
pomc	-1.40180	-8.378	0.0560	-1.21781	-1.557	0.0963	-0.64112	-10.089	0.1300
	$P > 0.05$	$P < 0.02$	$P > 0.05$	$P > 0.05$	$P > 0.02$	$P < 0.01$	$P > 0.05$	$P < 0.02$	$P > 0.05$
rag1	-1.21313	-7.542	0.0534	0.21337	0.346	0.1401	-0.13712	-0.421	0.1331
	$P > 0.05$	$P < 0.02$	$P > 0.05$	$P > 0.05$	$P > 0.02$	$P > 0.05$	$P > 0.05$	$P > 0.02$	$P > 0.05$
rag2	-1.77022	-82.555	0.0335	-0.12593	-1.420	0.1044	-0.65881	-8.246	0.0910
	$P < 0.05$	$P < 0.02$	$P < 0.05$	$P > 0.05$	$P > 0.02$	$P > 0.05$	$P > 0.05$	$P = 0.02$	$P > 0.05$
rho	-1.37952	-1.467	0.1000	0.65931	-0.801	0.1846	0.89497	-0.346	0.1582
	$P > 0.05$	$P > 0.02$	$P > 0.05$	$P > 0.05$	$P > 0.05$	$P > 0.05$	$P > 0.05$	$P > 0.02$	$P > 0.05$

Table S1.7 Extended Bayesian Skyline Plot (EBSP) results for sooglossid populations. Results are the 95% highest posterior density (HPD) interval for population size changes from all loci in a combined analyses. Constant population size cannot be rejected if the 95% HPD interval includes 0. Plus sign ([+]) indicates population expansion. Low sample sizes can lead to unreliable EBSP results (Heller & Siegismund, 2013) and consistent ESS values were not obtained for the Silhouette population of *Se. gardineri* until we removed underrepresented loci (*pomc*, *rag1*, *rho*).

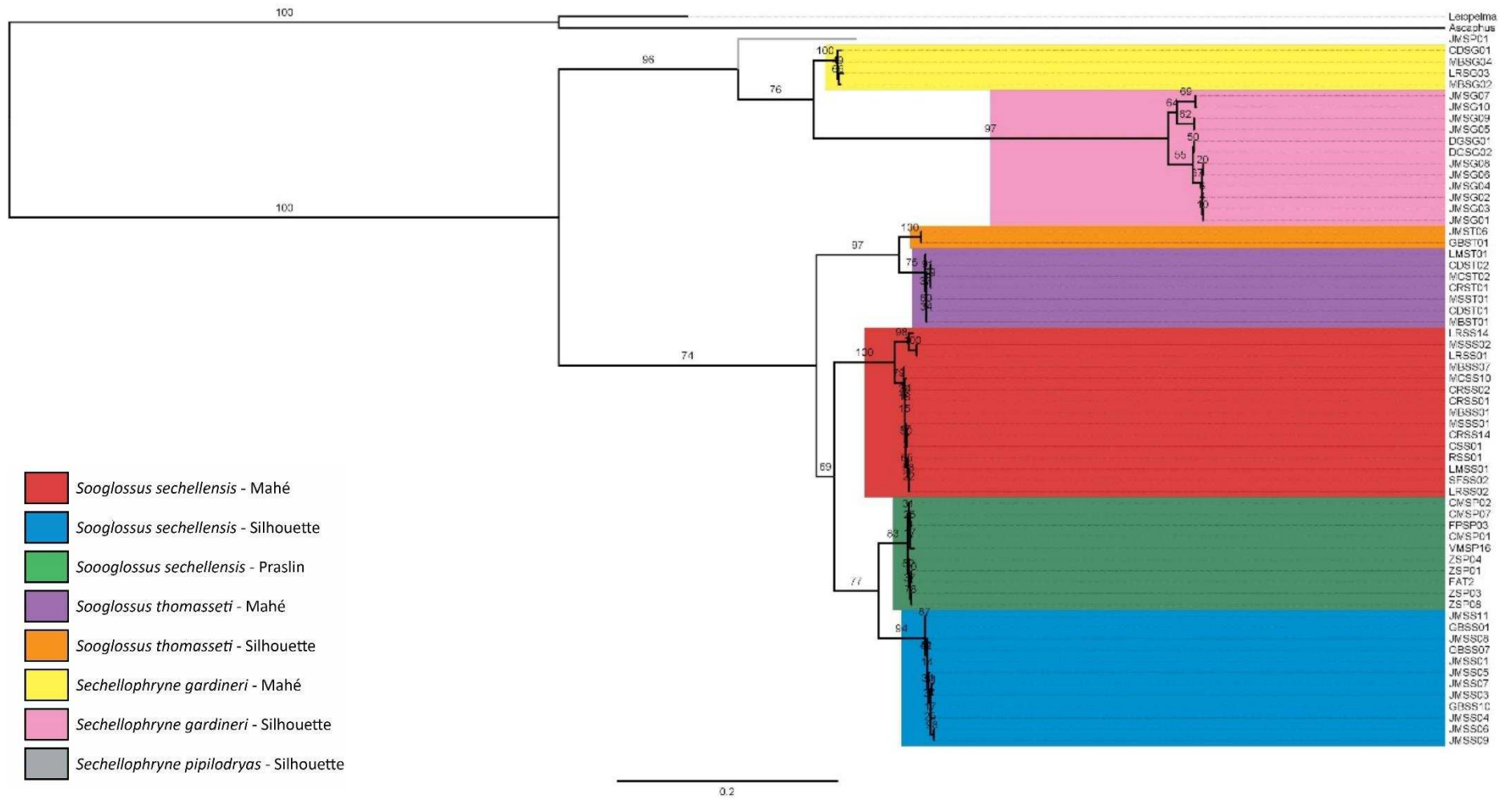|	*Sooglossus sechellensis*			*Sooglossus thomasseti*		*Sechellophryne gardineri*	
Island	Mahé	Praslin	Silhouette	Mahé	Silhouette	Mahé	Silhouette
Chain length	3×10^8	2×10^8	5×10^7	1×10^8	7.5×10^7	5×10^7	5×10^7
EBSP	[0, 3]	[1, 3][+]	[0, 3]	[0, 3]	[0, 3]	[0, 3]	[0, 2]

Figure S1.1 Maximum likelihood inferred mitochondrial DNA phylogeny of the Sooglossidae. Leiopelmatoidea (*Leiopelma+Ascaphus*) rooted outgroup. Branch support is indicated by maximum likelihood bootstrap (BS) values. Scale bar indicates substitutions per site.
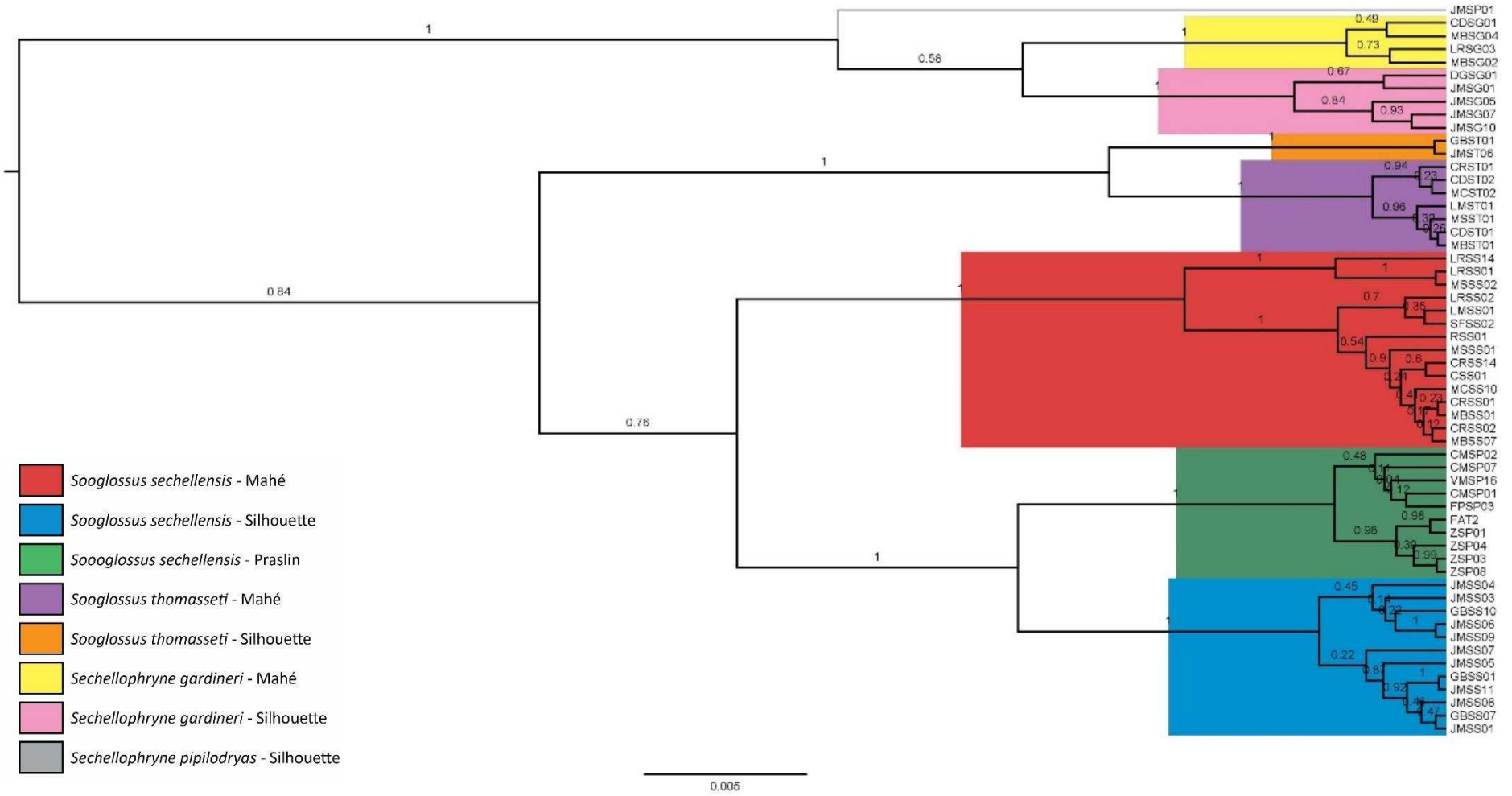
Figure S1.2 Bayesian inferred mitochondrial DNA phylogeny of the Sooglossidae using the Yule tree prior in BEAST2. Branch support is indicated by Bayesian Posterior Probabilities (PP). Scale bar indicates substitutions per site.
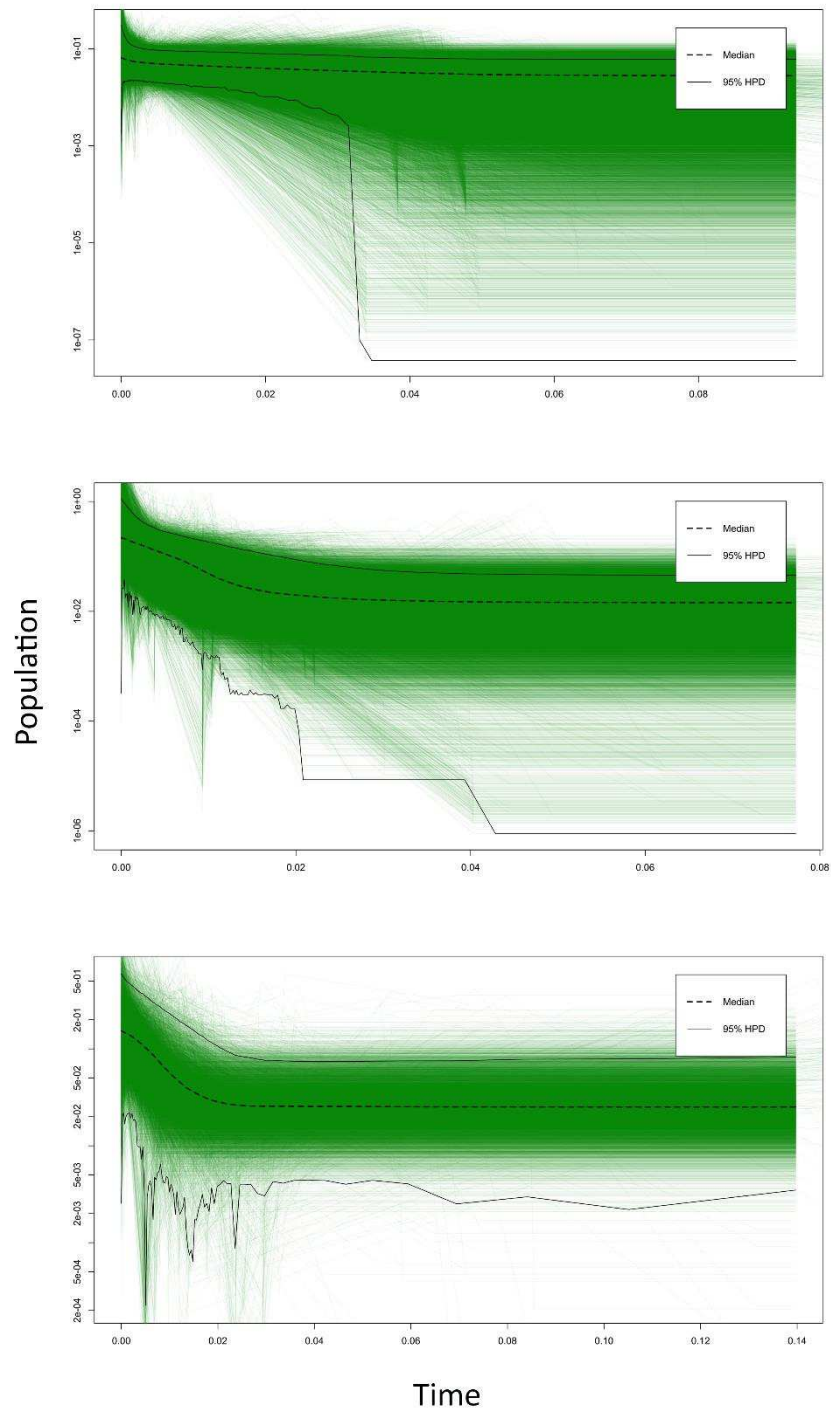
Figure S1.3 Extended Bayesian Skyline Plots of population size through time for *Sooglossus sechellensis*. The full view of the posterior all of the samples that are summarised by the median and 95% HPD interval are shown for the Mahé (top), Praslin (centre), and Silhouette (bottom) populations. The Praslin frogs are the only sooglossid population to reject a constant population size. EBSP analyses comprised all six loci. Time on x-axis in millions of years. Population size on y-axis in millions of years assuming a generation time of one year.
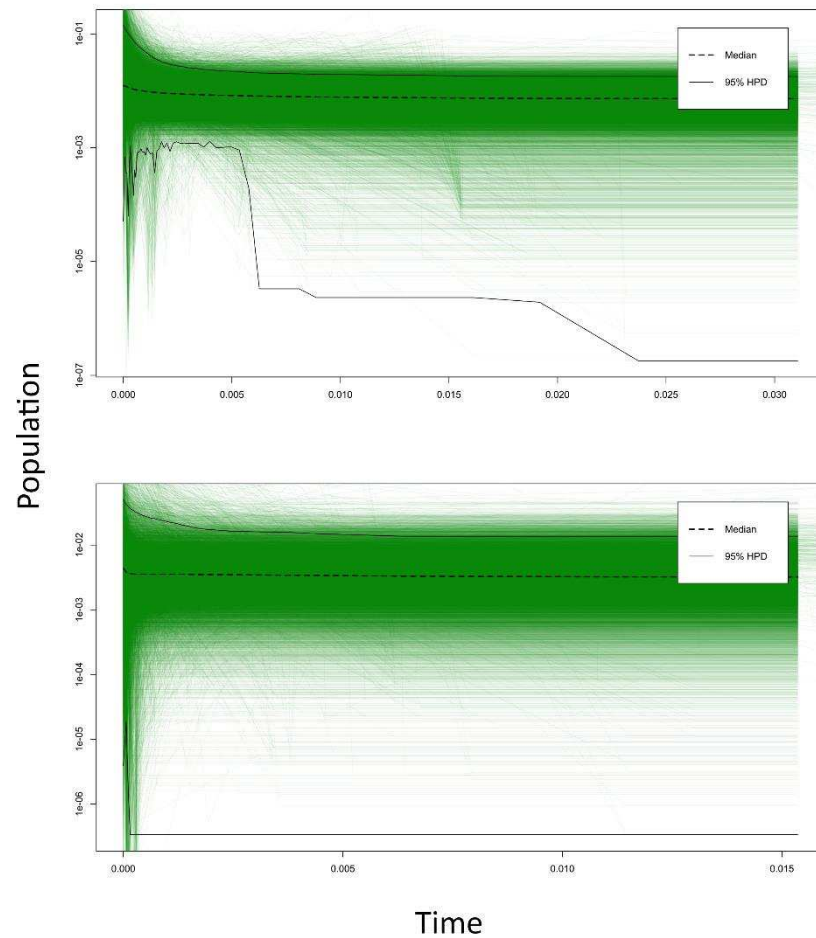
Figure S1.4 Extended Bayesian Skyline Plots of population size through time for *Sooglossus thomasseti*. The full view of the posterior all of the samples that are summarised by the median and 95% HPD interval are shown for the Mahé (top) and Silhouette (bottom) populations. EBSP analyses comprised all six loci. Time on x-axis in millions of years. Population size on y-axis in millions of years assuming a generation time of one year.
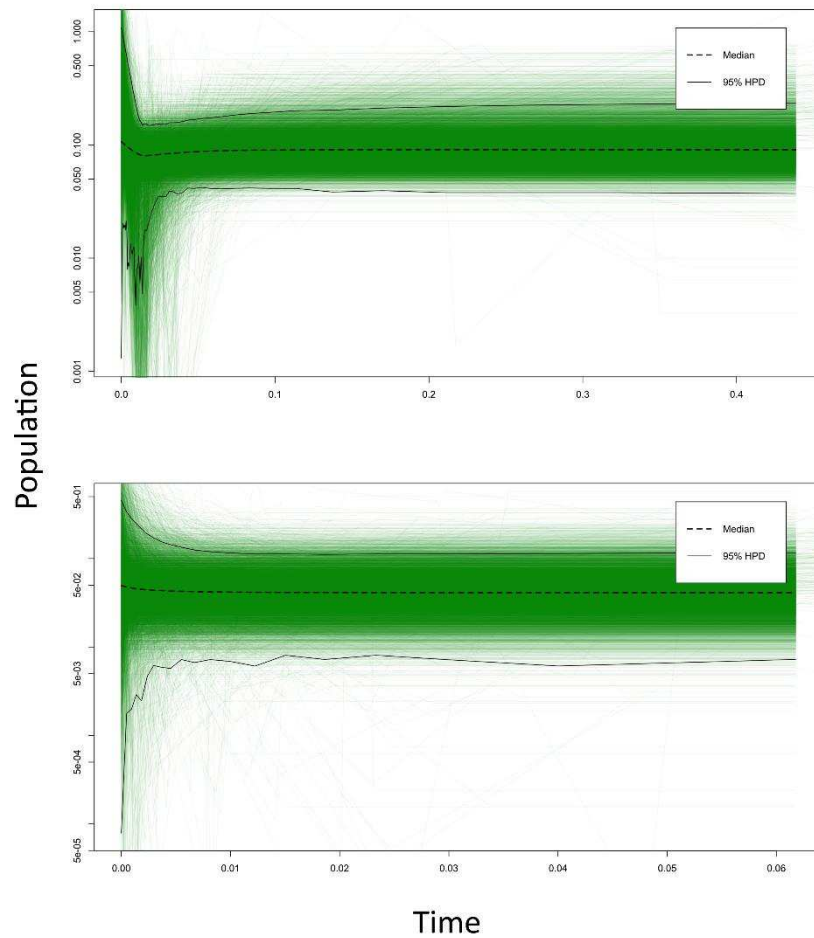
Figure S1.5 Extended Bayesian Skyline Plots of population size through time for *Sechellophryne gardineri*. The full view of the posterior all of the samples that are summarised by the median and 95% HPD interval are shown for the Mahé (top) and Silhouette (bottom) populations. EBSP analyses of the Mahé population comprised all six loci. Analyses of the Silhouette population comprised two loci (*16s*, *rag2*). Time on x-axis in millions of years. Population size on y-axis in millions of years assuming a generation time of one year

References

Biju SD, Bossuyt F. 2003. New frog family from India reveals an ancient biogeographical link with the Seychelles. *Nature* **425:** 711-714.

Bossuyt F, Milinkovitch MC. 2000. Convergent adaptive radiations in Madagascan and Asian ranid frogs reveal covariation between larval and adult traits. *Proceedings of the National Academy of Sciences* **97:** 6585-6590.

Chiari Y, Vences M, Vieites DR, Rabemananjara F, Bora P, Ramilijaona Ravoahangimalala O, Meyer A. 2004. New evidence for parallel evolution of colour patterns in Malagasy poison frogs (*Mantella*). *Molecular Ecology* **13:** 3763-3774.

Heller R, Chikhi L, Siegismund HR. 2013. The confounding effect of population structure on Bayesian skyline plot inferences of demographic history. *PLoS One* **8:** e62992.

Jukes TH, Cantor CR. 1969. Evolution of protein molecules. In: Munro HN, ed. *Mammalian protein metabolism*. New York.: Academic Press. 21-132.

Lanfear R, Calcott B, Ho SY, Guindon S. 2012. Partitionfinder: combined selection of partitioning schemes and substitution models for phylogenetic analyses. *Molecular Biology and Evolution* **29:** 1695-1701.

Palumbi S, Martin A, Romano S, McMillan WO, Stice L, Grabowski G. 1991. *The simple fool's guide to PCR*. Dept. of Zoology and Kewalo Marine Laboratory, University of Hawaii: Honolulu, HI.

Tamura K, Stecher G, Peterson D, Filipski A, Kumar S. 2013. MEGA6: Molecular Evolutionary Genetics Analysis version 6.0. *Molecular Biology and Evolution* **30:** 2725-2729.